Article

Discovery and Optimization of 3-(2-(Pyrazolo[1,5-a]pyrimidin-6-yl)ethynyl)benzamides as Novel Selective and Orally Bioavailable Discoidin Domain Receptor 1 (DDR1) Inhibitors

Ke Ding, Mingshan Gao, Duan Lei, Jinfeng Luo, Lianwen Zhang, Xiaoyun Lu, Yan Zhang, zhang zhang, zhengchao Tu, Yong Xu, and Xiaomei Ren

J. Med. Chem., **Just Accepted Manuscript** • DOI: 10.1021/jm301824k • Publication Date (Web): 22 Mar 2013

Discovery and Optimization of 3-(2-(Pyrazolo[1,5-a]pyrimidin-6-yl)ethynyl)benzamides as Novel Selective and Orally Bioavailable Discoidin Domain Receptor 1 (DDR1) Inhibitors

Mingshan Gao, [ω,ξ,δ] *Lei Duan,* [ω,δ] *Jinfeng Luo,* [ω] *Lianwen Zhang,* [ω] *Xiaoyun Lu,* [ω] *Yan Zhang,* [ω] *Zhang Zhang,* [ω] *Zhengchao Tu,* [ω*] *Yong Xu,* [ω] *Xiaomei Ren,* [ω] *and Ke Ding* [ω*]

[ω] Institute of Chemical Biology, Guangzhou Institutes of Biomedicine and Health, Chinese Academy of Sciences, #190 Kaiyuan Avenue, Guangzhou 510530, China

[ξ] University of Chinese Academy of Sciences, # 19 Yuquan Road, Beijing 100049, China

[δ] These authors contributed equally to this work.

*Corresponding authors: Tel: +86-20-32015276. Fax: +86-20-32015299.

E-Mail: ding_ke@gibh.ac.cn or tu_zhengchao@gibh.ac.cn

RECEIVED DATE (to be automatically inserted after your manuscript is accepted if required according to the journal that you are submitting your paper to)

ABSTRACT. Discoidin Domain Receptor 1 (DDR1) is an emerging potential molecular target for new anticancer drug discovery. We have discovered a series of 3-(2-(pyrazolo[1,5-a]pyrimidin-6-yl) ethynyl)benzamides that are selective and orally bioavailable DDR1 inhibitors. The two most promising

compounds (**7rh** and **7rj**) inhibited the enzymatic activity of DDR1 with IC_{50} values of 6.8 and 7.0 nM, respectively, but were significantly less potent in suppressing the kinase activities of DDR2, Bcr-Abl and c-Kit. Further study revealed that **7rh** bound with DDR1 with K_d value of 0.6 nM, while was significantly less potent to the other 455 kinases tested. The S(35) and S(10) selectivity scores of **7rh** were 0.035 and 0.008, respectively. The compounds also potently inhibited the proliferation of cancer cells expressing high levels of DDR1 and strongly suppressed cancer cell invasion, adhesion and tumorigenicity. Preliminary pharmacokinetic studies suggested that they possessed good PK profiles, with oral bioavailabilities of 67.4% and 56.2%, respectively.

KEYWORDS: Discoidin Domain Receptor 1, inhibitor, invasion, adhesion, tumorigenicity

INTRODUCTION

Discoidin Domain Receptors (DDRs) are members of the transmembrane receptor tyrosine kinases (RTKs) super-family. They are distinguished from other RTKs by the presence of a discoidin motif in the extracellular domain. [1, 2, 3] Unlike typical RTKs that use peptide-like growth factors as ligands, DDRs are activated by various types of triple-helical collagens, which are key components of the extracellular matrix (ECM). [4, 5] Two types of DDRs (DDR1 and DDR2) have been identified with distinct expression profiles and ligand specificities. DDR1 is widely expressed in epithelial cells in lung, kidney, colon and brain, whereas DDR2 is primarily expressed in mesenchymal cells including fibroblasts, myofibroblasts, smooth muscle and skeletal in kidney, skin, lung, heart and connective tissues. DDR1 is activated by all collagens tested to date (types I, II, III, IV, V, VIII and XI), while DDR2 is only activated by fibrillar collagens (collagen types I and III in particular). [3, 4, 5, 6] Collective evidences imply that that DDR1 and DDR2 play crucial roles in the regulation of fundamental cellular process, such as proliferation, survival, differentiation, adhesion, and matrix remodeling. [4, 7, 8] Dysregulation of DDR1 and DDR2 has been linked to a number of human diseases, including fibrotic disorders, atherosclerosis and cancer. [9, 10, 11] For instance, over-expression of DDR1 is associated with the poor prognosis in non-small cell lung cancer (NSCLC) [12] and is implicated in cell survival and

invasiveness in hepatocellular carcinoma, pituitary adenoma and prostate cancer. [13, 14, 15] High expression levels and/or mutation of DDRs are also frequently detected in the cancer cell lines and primary tumor tissues from lung, [16] breast, [17] brain, [18] ovary, [19] head and neck, [20] liver, [21] pancreas [22] and prostate. [15] Inhibition of DDR1 by small interfering RNA (siRNA) has been demonstrated to suppress tumorigenicity, inhibit lung cancer bone metastasis and increase cancer cell chemosensitivity. [23] Selective suppression of DDR2 also displayed promising antitumor activity in mouse xenografts of squamous lung cancer cells harboring a "gain-of function" mutation of DDR2. [24] Thus, DDR1 and DDR2 are considered as novel potential molecular targets for anticancer drug discovery.

Several small molecule Bcr-Abl inhibitors, imatinib (**1**), nilotinib (**2**), dasatinib (**3**), [23, 25, 27] bafetinib (**4**) [26] and ponatinib (**5**), [24, 27] have been reported to potently suppress the kinase activity of DDR1 and DDR2. These compounds also strongly inhibited the collagen-induced activation of DDR1 and DDR2 in HEK 293 cells, with IC_{50} values in low nanomolar ranges. [24] Given its promising therapeutic effect in mouse xenograft models, drug **3** has been selected for clinical investigation to treat squamous lung cancer (SCC) patients with mutated DDR2 (NCT01514864). [27] Sorafenib, a multiple-target drug used in the treatment of liver and renal cancer, was also reported to bind DDR1/DDR2 with nanomolar IC_{50} values. [27, 28] A thienopyridine derivative, LCB 03-0110, was recently found to inhibit collagen-induced autophosphorylation of DDR1 and DDR2, with IC_{50} values of 164 and 171 nM, respectively. [29] However, all of the reported DDR inhibitors displayed broad inhibition against a panel of many other kinases. New selective DDR1 and/or DDR2 inhibitors are highly desirable for further validating DDRs as drug targets.

In this paper, we report a series of 3-(2-(pyrazolo[1,5-a]pyrimidin-6-yl)ethynyl)benzamides as novel selective DDR1 inhibitors. The compounds potently suppressed the enzymatic activities of DDR1 with low nanomolar IC_{50} values but were markedly less potent against Bcr-Abl, DDR2 and c-Kit kinases. These compounds also strongly suppressed the proliferation of human cancer cells expressing high levels of DDR1, with IC_{50} values in the low micromolar range. Furthermore, the representative

compounds **7rh** and **7rj** potently suppressed cancer cell invasion, adhesion and tumorigenicity, indicating their potential to serve as new lead compounds for further anticancer drug discovery.

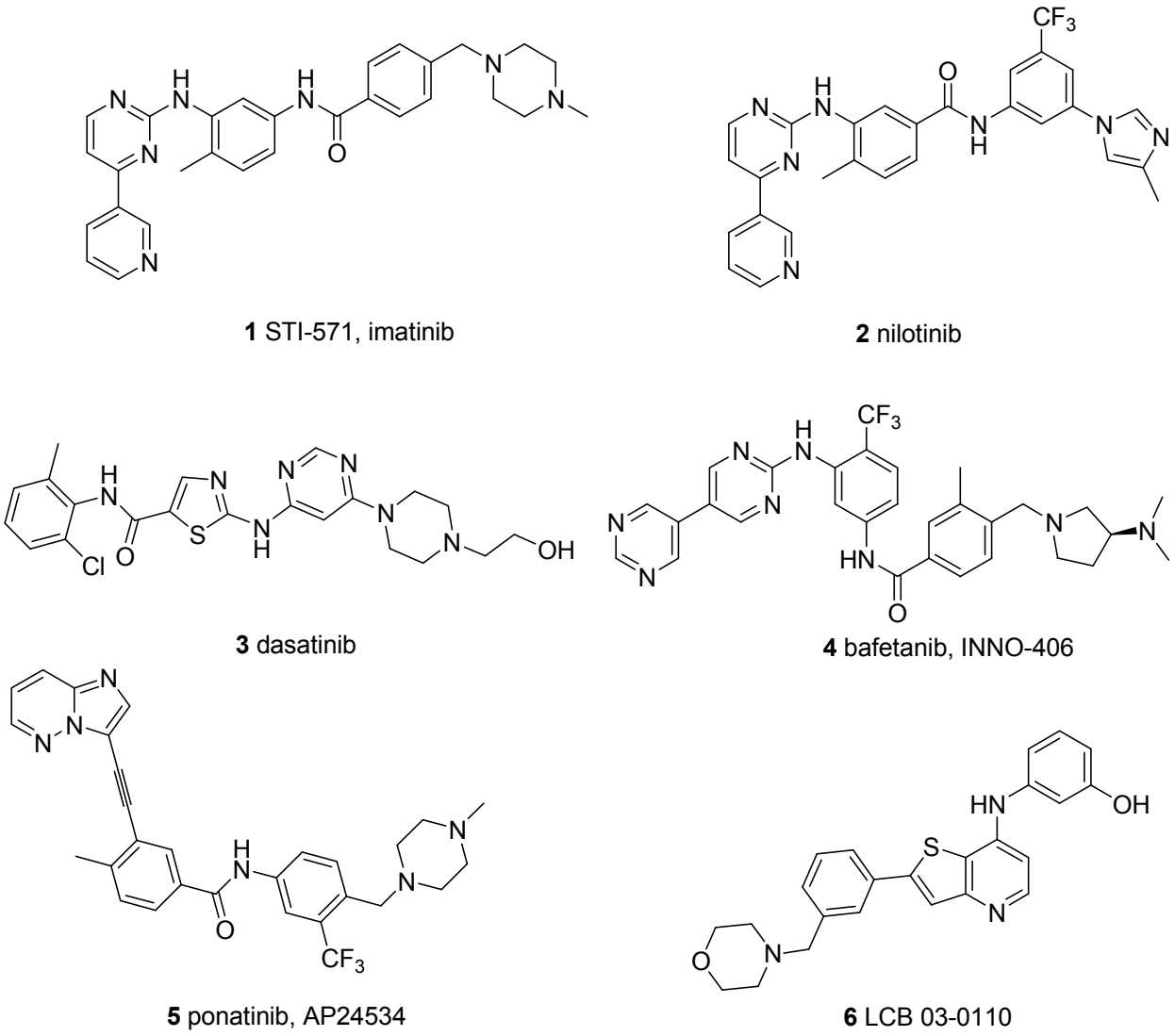

Figure 1. Chemical structures of reported non-selective DDR1 and DDR2 inhibitors.

CHEMISTRY

The new inhibitors were readily prepared using palladium-catalyzed Sonogashira coupling as the key steps (Scheme **1**). [30] Briefly, commercially available or newly prepared methyl 3-iodo-benzoates (**8**) were treated with ethynyltrimethylsilane under palladium catalysis to afford the Sonogashira coupling products, which were deprotected to produce the terminal alkynes **9**. The coupling of **9** with 6-bromopyrazolo[1,5-a]pyrimidine under Sonogashira conditions afforded the key intermediates **10**. The

esters **10** were hydrolyzed under basic conditions to yield the corresponding carboxylic acids **11,** which were coupled with various aryl amines to yield the desired inhibitors **7**.

Scheme 1. Syntheses of 3-(2-(pyrazolo[1,5-a]pyrimidin-6-yl)ethynyl)benzamide derivatives as new DDR inhibitors.

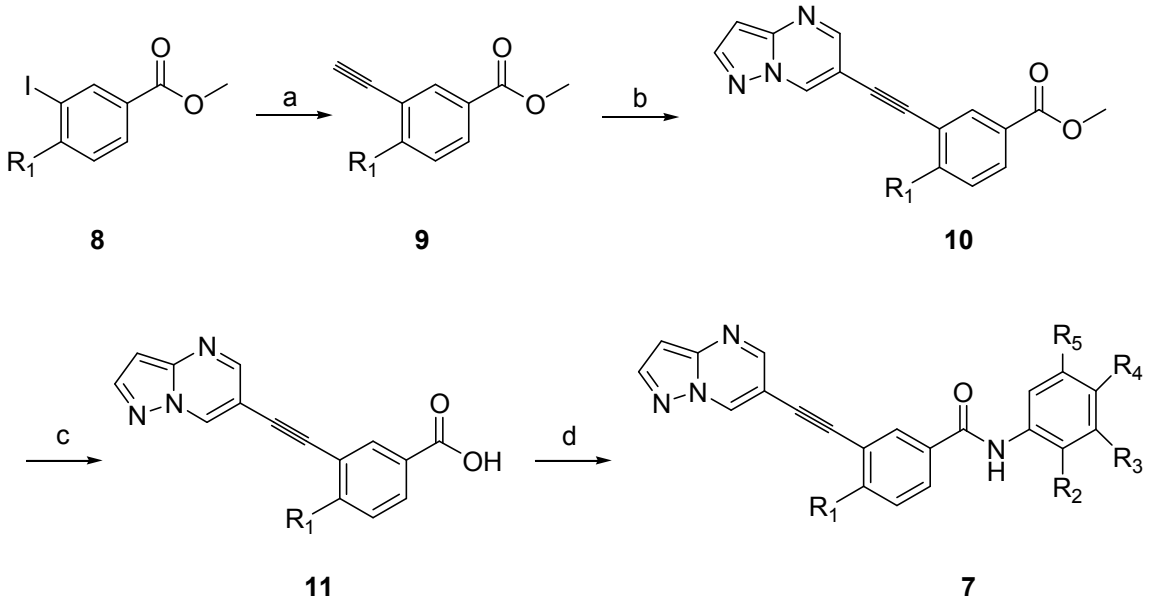

8 **9** **10** **11** **7**

Reagents and conditions: (a) i) trimethylsilyl acetylene, CuI, $PdCl_2(PPh_3)_2$, TEA, EtOAc, overnight, ~85.0%; ii) K_2CO_3, MeOH, 5 mins, 90.0-92.0%%; (b) CuI, $PdCl_2(PPh_3)_2$, NMP, 80 ℃, overnight, 80.0-85.0%; (c) NaOH, CH_3OH, H_2O, 50℃, 6 hrs, ~90.0%; (d) PyBOP, DIPEA, DCM, overnight, 40.0-90.0%.

RESULTS AND DISCUSSION

Almost all previously reported DDR inhibitors were originally developed as Bcr-Abl kinase suppressers. Furthermore, sequence alignment of human DDR1 and DDR2 demonstrated that they share ~61% sequence identity with Bcr-Abl in the ATP binding domain. [25d] Therefore, we initiated an effort to identify new DDR inhibitors by screening a library of approximately 2000 compounds that were originally designed as inhibitors of Bcr-Abl and other RTKs. Inhibition of DDR1 and DDR2 was first evaluated using the well-established LANCE ULTRA kinase assay. [31] For compounds with good inhibitory activity (IC_{50} below 100 nM) against DDR1 and/or DDR2, the inhibition of Bcr-Abl and c-Kit kinases was determined to investigate selectivity. Two reported inhibitors of both DDRs and Bcr-Abl (nilotinib (**2**) and dasatinib (**3**)) were included to validate the screening conditions. Under the

experimental conditions, **3** potently inhibited DDR1, DDR2 and Bcr-Abl with IC_{50} values of 4.8, 11.7 and 0.26 nM, respectively; these values were similar to previously reported data (Table **1**). [24, 25] The similar IC_{50} values of compound **2** with respect to previously reported data further confirmed the reliability of our screening methods. [25]

A number of compounds were found to exhibit strong inhibition of DDR1 and DDR2: *N*-isopropyl-4-methyl-3-(2-(pyrazolo[1,5-a]pyrimidin-6-yl)ethynyl) benzamide (**7a**) stood out because of its good activity and relatively high selectivity over Bcr-Abl. This compound potently inhibited the kinase activity of DDR1 with an IC_{50} value of 39.6 nM but did not detectably inhibit Bcr-Abl and DDR2 at 1.0 μM. However, further evaluation showed that this compound also strongly suppressed the activity of c-Kit, with an IC_{50} value of 67 nM.

Taking **7a** as a lead molecule, extensive structural optimization was conducted to improve its DDR-inhibitory activity and its selectivity over Bcr-Abl and c-Kit kinases. The results are summarized in Table **1** and Table **2**. We found that the isopropyl group in **7a** could be replaced with an n-butyl (**7b**), cyclohexyl (**7d**) or cyclopentyl (**7e**) moiety without reducing the inhibitory activity against DDR1. For instance, compound **7d** (with a cyclohexyl moiety) displayed an IC_{50} value of 29.1 nM against DDR1, which was similar to that of **7a**, but its inhibitory activity against c-Kit decreased approximately 3-fold. Interestingly, when the isopropyl group in **7a** was changed to an isobutyl moiety (**7c**), the inhibitory activity was dramatically decreased for all 4 of the tested kinases. Further investigation revealed that the isopropyl group in **7a** could also be replaced with a phenyl substituent (**7f**), which maintained strong inhibition of DDR1 and reduced the inhibition of c-Kit. Thus, compounds **7f** and **7a** displayed almost identical IC_{50} values against DDR1. However, the selectivity of **7f** for DDR1 over c-Kit kinase was approximately 12 times greater than that of **7a**.

Systematic structural optimization of **7f** revealed that substituents on the *N*-terminal phenyl ring dramatically impacted DDR1 kinase inhibition. For instance, when a methyl group was introduced at R_3 (**7h**), the IC_{50} was approximately 5.96 nM against DDR1, or 6.5 times more potent than **7f**. Although a methyl group at R_4 (**7i**) did not greatly influence the potency against DDR1, the R_2-methylated

compound **7g** was over 25-fold less potent than **7f**. The compounds featuring R_3-chloro (**7k**) or methoxy (**7n**) substituents were also significantly more potent than **7f** or the corresponding R_2- or R_4-substituted analogues (**7j**, **7l**, **7m** and **7o**). However, none of these compounds displayed marked selectivity for DDR1 over c-Kit kinase. Further studies suggested that the R_3 position could also tolerate Br (**7p**), I (**7q**), iso-propoxyl (**7t**), dimethylamino (**7u**), or 1-imidazolyl (**7v**) substituents while retaining good or moderate inhibition against DDR1. However, when a 1-(4-methyl)imidazolyl (**7w**) or (4-methylpiperazin-1-yl)methyl (**7x**) moiety was introduced at R_3, the potency was significantly decreased. Encouragingly, when R_3 was a CF_3 group, the resulting compound **7r** displayed a 6.14 nM IC_{50} value against DDR1 and 12–35-fold selectivity over DDR2, Bcr-Abl and c-Kit. By contrast, CF_3 substitution at R_4 (**7s**) almost totally abolished the inhibition of the 4 evaluated kinases, which confirmed that R_3 is the optimal position for structural optimization.

Table 1 *In vitro* inhibitory activities of compounds **7a-7x** against DDR1, DRR2, Bcl-Abl and c-Kit.[a, b]

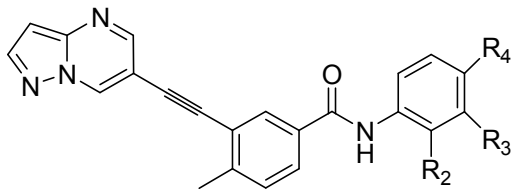

7

Compound	R_2	R_3	R_4	Kinase inhibition (IC_{50}, nM)			
				DDR1	DDR2	Bcr-Abl	c-Kit
7a	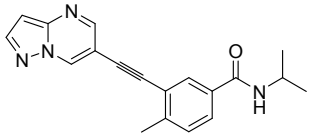			39.63	>1μM	>1μM	67
7b	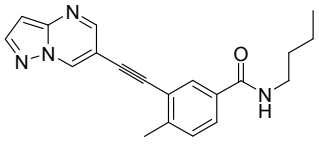			65.14	>1μM	>1μM	16.7

7c	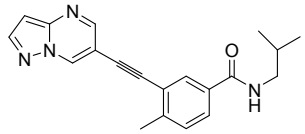			>1μM	>1μM	>1μM	497
7d	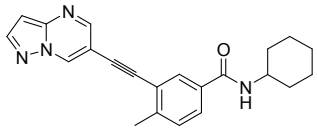			29.15	>1μM	>1μM	200
7e	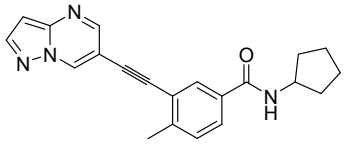			39.82	>1μM	>1μM	12.5
7f	H	H	H	38.90	>1μM	>1μM	457
7g	Me	H	H	>1μM	>1μM	>1μM	>1μM
7h	H	Me	H	5.96	>1μM	>1μM	3.03
7i	H	H	Me	47.75	>1μM	>1μM	2.61
7j	Cl	H	H	>1μM	>>1μM	>1μM	8320
7k	H	Cl	H	2.29	>1μM	>1μM	4.89
7l	H	H	Cl	>1μM	>1μM	>1μM	29.6
7m	MeO	H	H	470	>1μM	>1μM	82.3
7n	H	MeO	H	4.04	>1μM	>1μM	1.9
7o	H	H	MeO	22.36	>1μM	>1μM	9.28
7p	H	Br	H	16.64	>1μM	275.42	99.5
7q	H	I	H	19.75	>1μM	>1μM	254
7r	H	CF_3	H	6.14	73.84	97.44	214
7s	H	H	CF_3	>1μM	>1μM	>1μM	>1μM
7t	H	i-PrO	H	35.02	>1μM	>1μM	117

7u	H		H	9.72	>1μM	310.63	18.8
7v	H	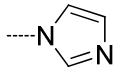	H	19.03	>1μM	198	82.4
7w	H	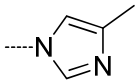	H	386.5	2270	159	284
7x	H	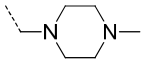	H	324.1	>1μM	504.0	257
2				32.6 (43) [c]	105 (55) [c]	43.5	N.D.
3				4.80 (0.5) [c]	11.7 (1.4) [c]	0.26	2.38

[a] DDR1 and DDR2 experiments were performed using LANCE ULTRA kinase assay according to the manufacturer's instructions. The data are means from at least 2 independent experiments. [b] Bcr-Abl and c-Kit activity experiments were performed using the FRET-based Z'-Lyte assay according to the manufacturer's instructions. The data are means from at least 3 independent experiments. [c] Reported data.[24, 25]

A series of R_3, R_5-disubstituted compounds was also designed and synthesized (Table **2**). R_3, R_5-Dimethyl compound **7y** displayed similar potency against DDR1 to that of the mono-methyl compound **7h** (Table **1**), but its selectivity was improved. The R_3-methyl, R_5-chloro compound **7z** also potently inhibited DDR1, with an IC_{50} of 29.8 nM. These results strongly suggested that one hydrophobic group in R_3 (or R_5) would be sufficient to interact with DDR1, whereas the other group might be located outside of the binding pocket, providing an ideal position for a pharmaceutically acceptable hydrophilic group to improve the hydrophilic-lipophilic balance of the molecule. Therefore, compounds **7ra**, **7re**, **7rf** and **7rg**, which featured hydrophilic 1-(4-methyl)imidazolyl, morpholinomethyl, piperidin-1-ylmethyl or (pyrrolidin-1-yl)methyl groups, respectively, were designed and synthesized. All compounds showed comparable inhibition of DDR1 to the mono-substituted lead compound **7r**. For instance, **7ra** displayed an IC_{50} of 8.93 nM against DDR1, while **7r** had a value of 6.14 nM. However, introduction of a hydrophilic group seemed to increase inhibition of Bcr-Abl, causing a significant loss

of DDR1 selectivity. Compounds **7rb**, **7rc** and **7rd** were also obvious less selective than the corresponding mono-substituted compounds **7h**, **7k** and **7n**, although their potencies against DDR1 were not significantly changed.

Table 2 *In vitro* inhibitory activities of compounds **7y-7rj** against DDR1, DRR2, Bcl-Abl and c-Kit.[a, b]

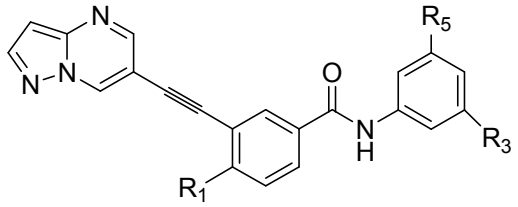

7

Compound	R_1	R_3	R_5	Kinase inhibition (IC_{50}, nM)			
				DDR1	DDR2	Bcr-Abl	c-Kit
7y	Me	Me	Me	6.34	116.0	>1μM	185
7z	Me	Me	Cl	29.81	>1μM	>1μM	>1μM
7ra	Me	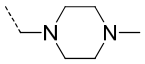	CF_3	8.93	100.56	16.2	756
7rb	Me	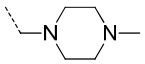	CH_3	6.71	37.1	38.9	274
7rc	Me	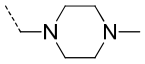	Cl	13.94	103	59.5	407
7rd	Me	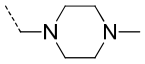	OMe	13.3	125	128	413
7re	Me	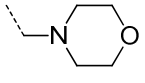	CF_3	17.49	775.9	129.1	>1μM
7rf	Me	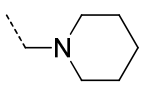	CF_3	37.58	214	115	>1μM

7rg	Me	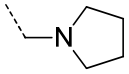	CF_3	12.47	131.36	49.04	741
7rh	Et	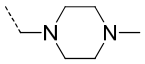	CF_3	6.811	101.4	355	>10μM
7ri	Cl	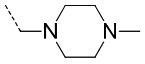	CF_3	10.05	172.65	54.7	1500
7rj	H	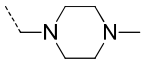	CF_3	7.02	93.65	447	243

[a] DDR1 and DDR2 experiments were performed using LANCE ULTRA kinase assay according to the manufacturer's instructions. The data are means from at least 2 independent experiments. [b] Bcr-Abl and c-Kit activity experiments were performed using the FRET-based Z'-Lyte assay according to the manufacturer's instructions. The data are means from at least 3 independent experiments.

Prior studies suggested that the "flag-methyl" R_1 group was important for AP24534 (**5**) and other inhibitors to maintain strong binding to Bcr-Abl kinase. [32] We hypothesized that Bcr-Abl inhibition might be decreased or eliminated by modifying the R_1 substituent. Indeed, although the R_1-Cl compound **7ri** showed similar potency and selectivity to that of **7ra**, we were pleased to find that the Bcr-Abl inhibitory potencies were significantly decreased by replacing the R_1-methyl group in **7ra** with an ethyl group (**7rh**) or a hydrogen atom (**7rj**); the activities against DDR1 and DDR2 remained unchanged. For instance, compound **7rh** inhibited DDR1 with an IC_{50} of 6.81 nM, while the IC_{50} values for DDR2, Bcr-Abl and c-Kit were 101.4, 355 and over 10,000 nM, respectively. Compound **7rj** also displayed 12–64-fold selectivity for DDR1 over the other 3 kinases evaluated. Thus, compounds **7rh** and **7rj** represented the two most potent and selective DDR1 inhibitors for further investigation.

The direct binding affinity of compound **7rh** with DDR1 kinase was determined by using an active-site-dependent competition binding assay (conducted by Ambit Bioscience, San Diego, USA). It was shown that compound **7rh** tightly bound to the ATP-binding sites of DDR1 with K_d values of 0.6 nM. We further profiled the compound against a panel of 456 kinases (including 395 non-mutated kinases) using the Ambit Kinome screening platform to investigate the selectivity of the new DDR1 inhibitor. The screening concentration was 100 nM which was about 160 times higher than its K_d values with

DDR1. The results clearly revealed that compound **7rh** displayed an excellent selective profile on DDR1 (Supporting Information and Table **3**.). For instance, compound **7rh** showed almost 100% competition rate (99.5% inhibition, Ctrl% = 0.05) with DDR1 at 100 nM, while it only displayed obvious binding (inhibition rate >65%, or Ctrl% < 35%) with 14 of the other 395 non-mutated kinases evaluated. These kinases included Abl1, B-Raf (V600E), DDR2, EPHA8, HCK, LOK, MAK, PDGFRβ, Tie2, TRKb, TRBc and ZAK etc. The S(35) and S(10) selectivity scores were 0.035 and 0.008, respectively.

Table 3 Hits with Ctrl% < 35% in a selectivity profiling study of compound **7rh** against 396 non-mutated kinases at 100 nM. [a]

Kinases	Ctrl% @ 100 M	S-score	
		S(35)	(S10)
Non-phosphorylated Abl-1	27	0.035	0.008
B-Raf (V600E)	29		
DDR1	0.05		
DDR2	28		
EPHA-8	21		
HCK	30		
GCN2	25		
LOK	1.6		
MAK	13		
PDGFRβ	31		
Tie2	31		
TRBb	8.7		
TRBc	12		
ZAK	22		

[a] The binding rates of **7rh** with different kinases were determined by using an active-site-dependent competition binding assay (conducted by Ambit Bioscience, San Diego, USA). The results were reported as "control%" (ctrl%), where lower numbers indicate stronger binding. S-core = number of hits

/ numbers of assays. Ctrl% = (test compound signal – positive control signal) / (negative control signal – positive control signal) ×100. Wherein, negative control = DMSO (Ctrl% = 100%); positive control = control compound (Ctrl% = 0%). S-score (selectivity score) = number of hits / number of assays. S(35) = (number of non-mutated kinases with ctrl% < 35%) / (number of non-mutated kinases tested). S(10) = (number of non-mutated kinases with ctrl% < 10%) / (number of non-mutated kinases tested).

To further validate these new DDR1 inhibitors, we examined the effects of the representative compounds **7rh** and **7rj** on the activation of DDR1 and downstream signals in NCI-H23 non-small cell lung cancer cells (NSCLC) expressing high level of DDR1; the results are summarized in Figure **2**. It was clear that both compounds inhibited phosphorylation of DDR1 in a dose-dependent manner. It has previously been demonstrated that DDR1 activation can trigger pro-survival Ras/Raf/Erk and PI3K/Akt signals, resulting in enhanced expression of DDR1 and the anti-apoptotic Bcl-xL. [33] Not surprisingly, the inactivation of DDR1 by compounds **7rh** and **7rj** induced significant decrease of total protein levels of DDR1 and Bcl-xL. Prior studies have also revealed that DDRs stimulate the production of matrix metalloproteinase (MMP). [33] Indeed, inhibition of DDR1 by **7rh** and **7rj** caused a significant reduction in the level of MMP-2. However, the effect on MMP-9 was less obvious.

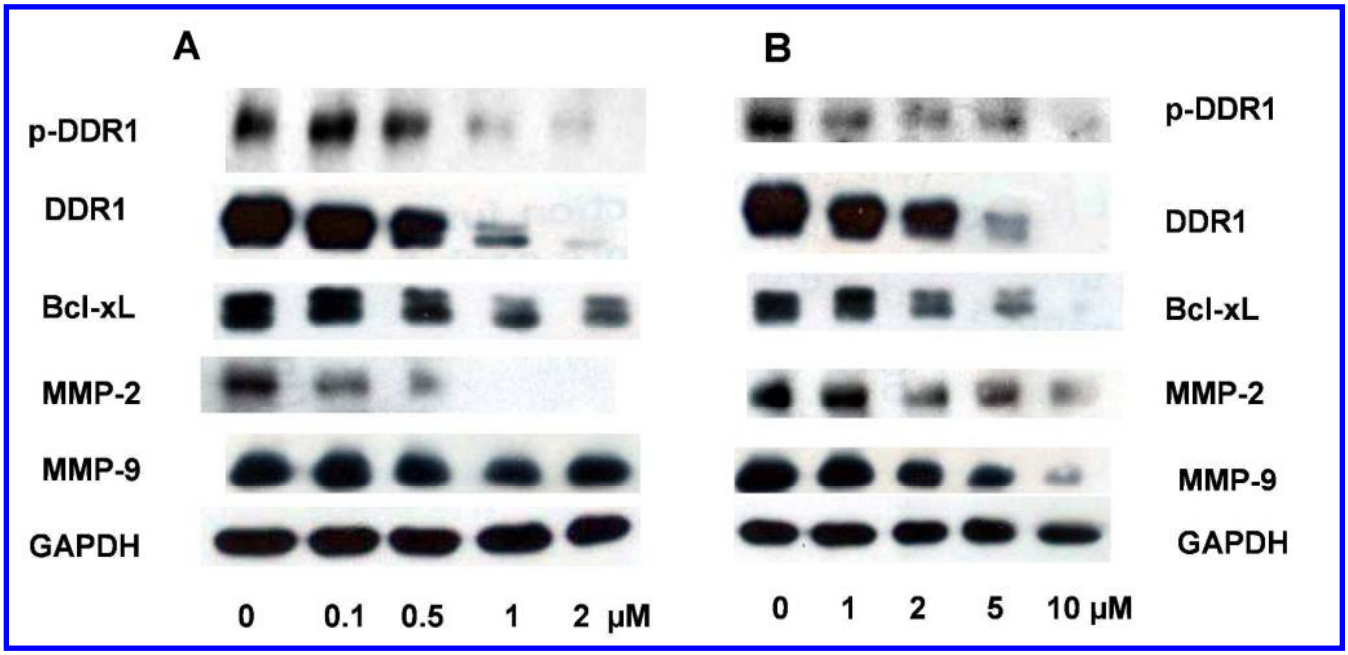

Figure 2. Compounds **7rh** and **7rj** inhibit both the expression and phosphorylation of DDR1 and downstream signaling in a dose-dependent manner. A) Compound **7rh** inhibits the expression and phosphorylation of DDR1 and downstream signaling in NCI-H23 NSCLC cells; B) Compound **7rj** inhibits the expression and phosphorylation of DDR1 and downstream signaling in NCI-H23 NSCLC cells.

The anti-proliferative effects of compounds **7rh** and **7rj** were also investigated using a panel of cancer cell lines expressing high levels of DDR1 (Table **4**). The drugs **2** and **3** were included as positive controls because of their strong DDR1/DDR2 inhibitory activities. The cancer cell lines included A549, NCI-H23 and NCI-H460 human NSCLC cells; MDA-MB-435S, MCF-7 and T47D human breast cancer cells; HCT116 human colon cancer cells; and K562 chronic myelogenous leukemia cells. It was also noteworthy that the cells have been successfully used as models for the functional investigation on DDR1. [23, 39c, 39d, 43] As shown in Table **3**, compounds **7rh** and **7rj** potently inhibited proliferation, with IC_{50} values in the low μM range. For instance, compound **7rh** suppressed the growth of A549, NCI-H23 and NCI-H460 human NSCLC cells with IC_{50} values of 2.7, 2.1 and 3.0 μM, respectively, while the value in K562 human CML cells was approximately 0.038 μM. The strong inhibition of **7rh** and **7rj** on K562 cell growth might be, at least in part, due to the high level of activated DDR1 (Supporting Information). Further investigation also revealed that the compounds induced apoptosis of NCI-H23 NSCLC cells in a dose-dependent manner (see Supporting Information).

Table 4. The anti-proliferative effects of compounds **7rh** and **7rj** on a panel of cancer cells harboring high levels of DDR1.

compound	Anti-proliferative activity (IC_{50}, μM) [a]							
	A549 [b]	NCI-H23 [b]	NCI-H460 [b]	MDA-MB-435S [b]	MCF-7 [b]	T47D [b]	HCT116 [b]	K562 [c]
7rh	2.74±0.22	2.08±0.12	2.98±0.57	2.22±0.05	2.15±0.04	1.88±0.22	1.13±0.18	0.038±0.011
7rj	11.73±0.49	11.91±0.28	7.77±0.95	2.86±0.07	2.82±0.18	3.13±0.14	2.41±0.18	0.059±0.005
2	6.63±0.45	3.05±0.45	14.41±2.31	2.66±0.211	6.92±1.03	6.08±0.01	2.39±0.02	0.015±0.003 [d]
3	12.66±1.12 (>1.0) [e]	2.27±0.44 (1.02) [e]	8.99±0.71	3.90±0.05 (7.78) [e]	2.57±0.08 （12.4） [e]	0.90±0.20 (0.45) [e]	2.30±0.01 (4.45) [e]	0.0007±0.0001 [d]

[a] Data are means from at least 4 independent experiments. [b] The anti-proliferative activities of the compounds were evaluated using an MTT assay. [c] IC_{50} values were determined by using the cell counting kit (CCK-8) assay. [d] The potent antiproliferative activity might be due to strong inhibition against Bcr-Abl. [e] Reported data. [42]

MMP2 and MMP9 are key enzymes mediating the degradation of extracellular matrix (ECM), which is a critical step in metastasis. Increased levels of MMP2 and MMP9 have been associated with metastasis of different types of solid tumor. [35, 36] Collectively, the studies demonstrate that DDR1 stimulates the production of MMPs. [4, 34] Our results clearly demonstrate that **7rh** and **7rj** potently decrease MMPs (Figure **2**), suggesting that DDR1 inhibitors may inhibit the migration and invasion of cancer cells. Therefore, we investigated the effects of **7rh** and **7rj** on the invasiveness of NCI-H23 NSCLC cells using a Boyden chamber assay.[37] Matrigel was applied to the filter membrane, and the number of NCI-H23 cells that penetrated the matrigel and membrane was quantified. As shown in Figure **3**, compounds **7rh** and **7rj** inhibited the invasiveness of NCI-H23 cells in a dose-dependent manner. Treatment with **7rh** at 1.0, 2.0 or 5.0 μM for 24 hours inhibited invasion by ~30%, ~37% or ~82%, respectively ($P<0.01$, compared to vehicle control; see Figure **3A** and Supporting Information). The corresponding numbers for **7rj** were 36%, 39% and 57%, respectively (Figure **3B** and Supporting Information). These results strongly suggested that the compounds may suppress the metastasis of NSCLC cancers.

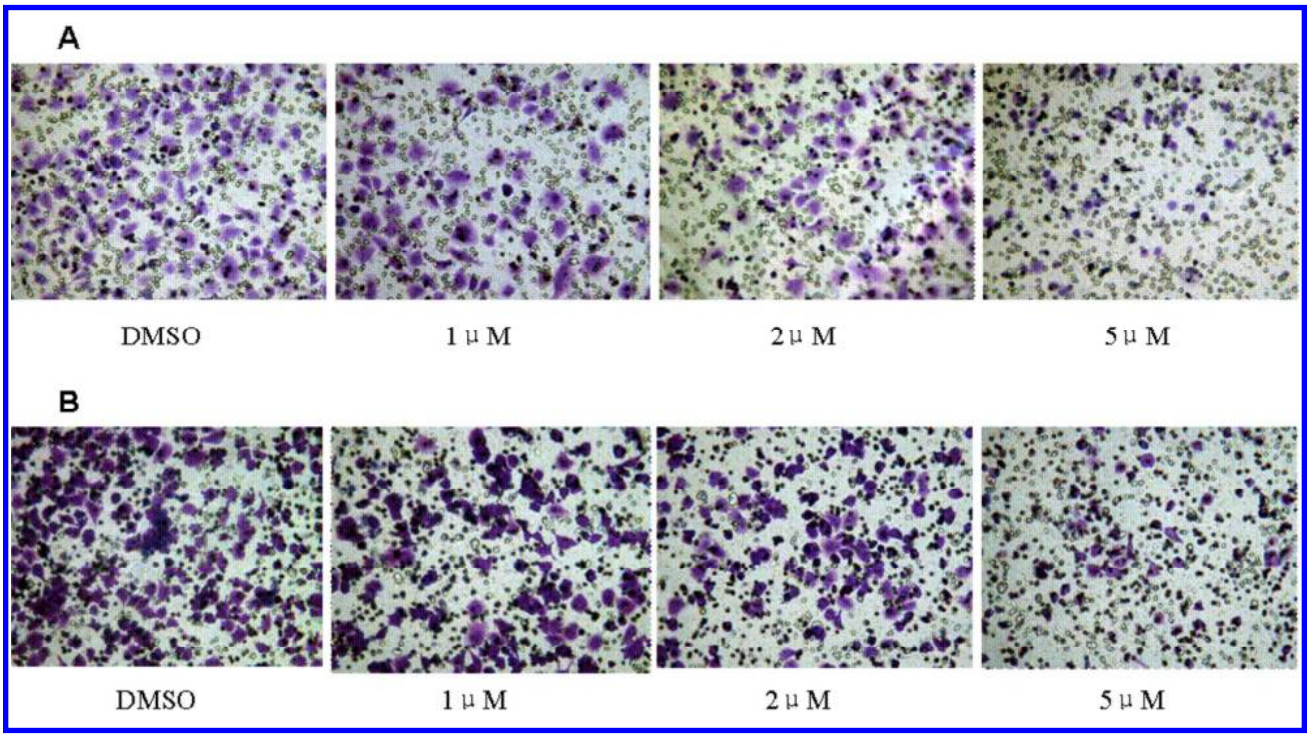

Figure 3. Compounds **7rh** and **7rj** inhibit the invasion of NCI-H23 NSCLC cells in a dose dependent manner. A) Compound **7re** inhibits the invasion of NCI-H23 NSCLC cells in a Boyden chamber assay. B) Compound **7rj** inhibits the invasion of NCI-H23 NSCLC cells in a Boyden chamber assay. The results are representative of two independent experiments.

Cell adhesion involves a number of regulatory processes, including growth, differentiation, proliferation, migration and regeneration. Adhesion is crucial in the formation and maintenance of coherent multicellular structures.[38] DDR1 has been implied as one of the key regulators of cell adhesion.[39] Therefore we investigated the impact of **7rh** and **7rj** on cell-matrix adhesion using a well-established crystal violet adhesion assay.[40] NCI-H23 NSCLC cells adhering to the pre-coated BD Matrigel were treated with **7rh** and **7rj** in different concentrations. As shown in Figure **4**, compounds **7rh** and **7rj** potently inhibited cell-matrix adhesion in a dose-dependent manner. Treatment with **7rh** at 5.0, 10.0 or 20.0 μM for 2 hours inhibited cell-matrix adhesion by ~17%, ~40% or ~88%, respectively, compared to vehicle control (Figure **4A**)

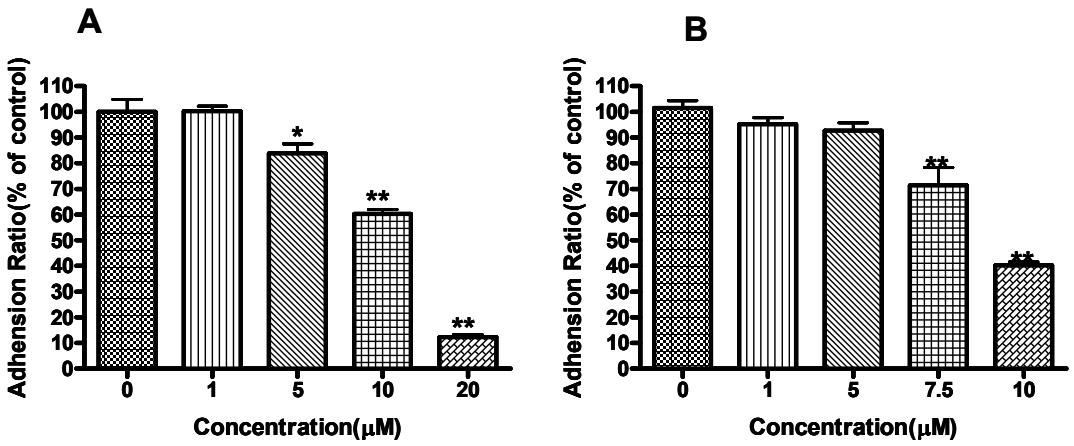

Figure 4. Compounds **7rh** and **7rj** inhibit the cell-matrix adhesion of NCI-H23 cells in a crystal violet adhesion assay. A) Compound **7rh** inhibits the cell-matrix adhesion of NCI-H23 cells in a dose dependent manner. B) Compound **7rj** inhibits the cell-matrix adhesion of NCI-H23 cells in a dose dependent manner. The results are representative of 2 independent experiments. (* $p<0.05$, ** $p<0.01$)

The effects of **7rh** and **7rj** on the tumorigenicity of NCI-H23 cancer cells were also examined using an *in vitro* colony formation assay, as well as anchorage-independent growth in soft agarose. As shown in Figures **5**A and **5B**, the compounds inhibited colony formation by NCI-H23 NSCLC cells in a dose-dependent manner, with IC_{50} values of 0.56 and 3.29 μM, respectively (Supporting Information). Anchorage-independent growth of cells in soft agar is one of the hallmarks of cellular transformation and uncontrolled cell growth. Therefore, the anti-tumorigenic effects of **7rh** and **7rj** on NCI-H23 cancer cells were further evaluated using a 3-dimensional (3D) soft-agar assay, which is closer to the *in vivo* cellular environment. The results (Figure **5C)** reveal that the compounds potently reduce the number and size of colonies, suggesting strong inhibition of cancer cell transformation.

Given their promising *in vitro* biological activities, preliminary *in vivo* pharmacokinetic (PK) studies of **7rh** and **7rj** were also conducted in rats. The results are summarized in Table **5**. Compounds **7rh** and **7rj** displayed good pharmacokinetic properties, with oral bioavailability of 67.4% and 56.2%, respectively. **7rh** and **7rj** also possessed reasonable half-lives of 15.5 and 9.8 hours, respectively, after oral administration.

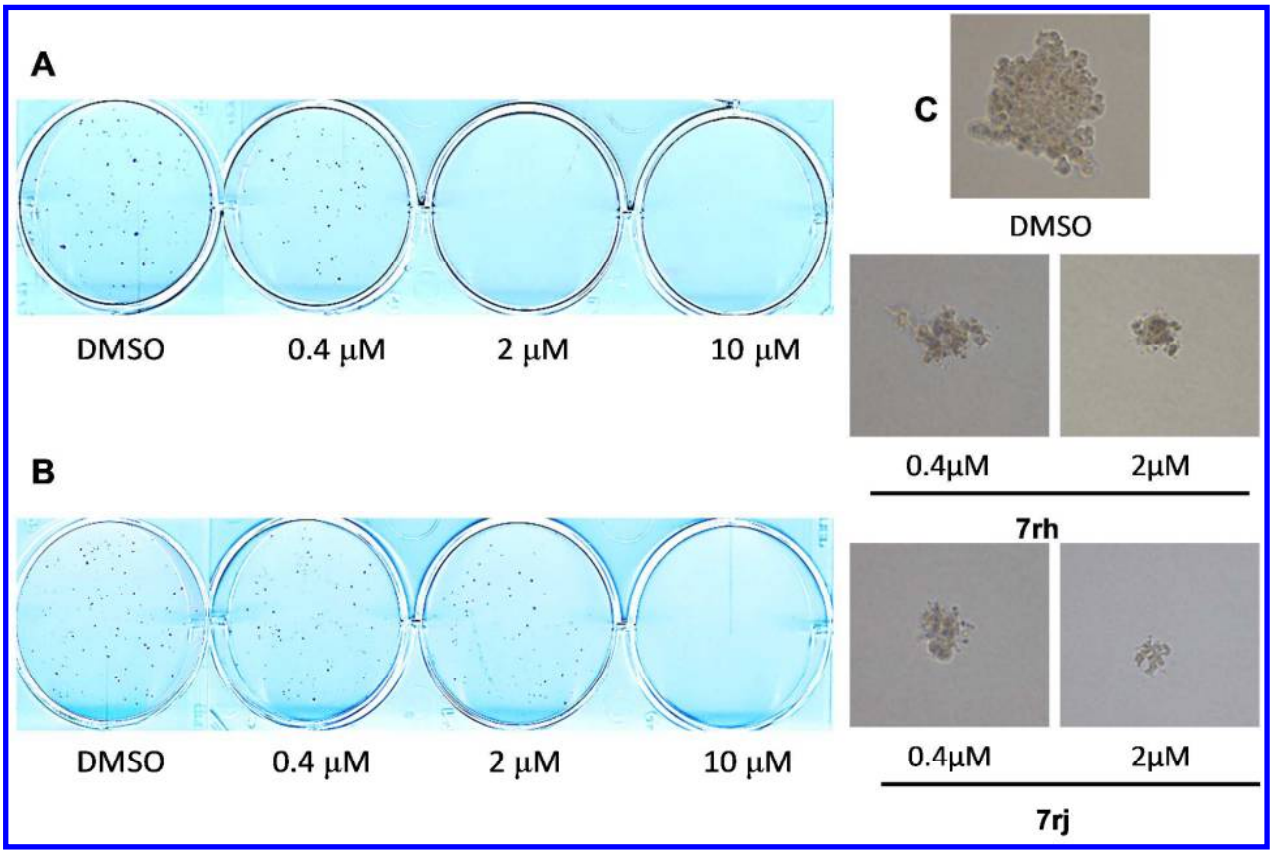

Figure 5. Compounds **7rh** and **7rj** suppress NCI-H23 cell tumorigenicity. A) Compound **7rh** inhibits NCI-H23 cancer cell colony formation in a colongenic assay. B) Compound **7rj** inhibits NCI-H23 cancer cell colony formation in a clonogenic assay. C) **7rh** and **7rj** reduce the number and size of colonies of NCI-H23 cancer cells in a soft agar cell transformation assay. The results are representative of 2 independent experiments.

Table 5. Compounds **7rh** and **7rj** display a good pharmacokinetic profile in rats. [a]

	7rh		**7rj**	
	Oral (25 mg/kg)	i.v. (5 mg/kg)	Oral (25 mg/kg)	i.v. (5 mg/kg)
$AUC_{(0-\infty)}$ (μg/L*h)	37587.54±3453.28	11156.31±921.89	24706.67±4079.71	8799.33±2550.47
$T_{1/2}$ (h)	15.53±1.58	13.21±1.48	9.80±4.72	7.55±3.47
T_{max} (h)	4.25±1.26	0.033	4.00±1.41	0.033
C_{max} (μg/L)	1867.50±118.43	1122.50±97.40	1767.50±216.39	1235.00±68.56
F (%)	67.4%		56.2%	

[a] SD rats (male, 4 animals per group) weighted 180~220g were used for the study.

In summary, a series of 3-(2-(pyrazolo[1,5-a]pyrimidin-6-yl)ethynyl)benzamides were found to be selective small molecule DDR1 inhibitors. The compounds potently inhibited DDR1 but were significantly less potent against many other kinases such as DDR2, Abl and c-Kit. The most promising

compounds **7rh** and **7rj** displayed nanomolar IC_{50} values against DDR1 and potently inhibited the proliferation of a panel of cancers cell lines expressing high levels of DDR1, including A549, NCI-H23, NCI-H460 human NSCLC cells; MDA-MB-435S, MCF-7, T47D human breast cancer cells; HCT116 colon cancer cells; and K562 CML cells. These compounds also potently suppressed the activation of DDR1 and downstream signaling. Further investigation demonstrated that compounds **7rh** and **7rj** strongly inhibited invasiveness, cell-matrix adhesion and tumorigenicity in NCI-H23 human NSCLC cells. Moreover, in preliminary *in vivo* pharmacokinetic studies, **7rh** and **7rj** displayed excellent profiles. Our study provides new research probes and lays a basic foundation for further validation of DDR1 as a potential target for anticancer drug development.

EXPERIMENTAL

Chemistry. Reagents and solvents were obtained from commercial suppliers and used without further purification. Flash chromatography was performed using silica gel (300-400 mesh). All reactions were monitored by TLC, silica gel plates with fluorescence F_{254} were used and visualized with UV light. ^{1}H and ^{13}C NMR spectra were recorded on a Bruker AV-400 spectrometer at 400 MHz and Bruker AV-500 spectrometer at 125 MHz, respectively. Coupling constants (*J*) are expressed in hertz (Hz). Chemical shifts (δ) of NMR are reported in parts per million (ppm) units relative to internal control (TMS). The low or high resolution of ESI-MS was recorded on an Agilent 1200 HPLC-MSD mass spectrometer or Applied Biosystems Q-STAR Elite ESI-LC-MS/MS mass spectrometer, respectively. The purity of compounds was determined to be over 95% (>95%) by reverse-phase high performance liquid chromatography (HPLC) analysis. HPLC instrument: DIONEX SUMMIT HPLC (Column: Diamonsil C18, 5.0 μm, 4.6 x 250 mm(Dikma Technologies); Detector: PDA-100 Photodiode Array; Injector: ASI-100 Autoinjector; Pump: p-680A.). Elution: 85% MeOH in water; flow rate, 1.0 mL/min.

Methyl 3-ethynyl-4-methylbenzoate (9a) To a solution of methyl 3-iodo-4-methylbenzoate (27.61 g, 100 mmol) in EtOAc (300 mL) was added $Pd(PPh_3)_2Cl_2$ (0.70 g, 1 mmol), CuI (0.19 g, 1 mmol), and triethylamine (30.4 g, 300 mmol). The mixture was stirred at room temperature overnight under argon atmosphere. The reaction mixture was filtered through a pad of celite. The filtrate was concentrated and

the resulting residue was purified by flash chromatography to give methyl 4-methyl-3-((trimethylsilyl)ethynyl)benzoate as a white solid (20.9 g, 85.0%). ^{1}H NMR (400 MHz, DMSO-d_6) δ 7.89 (d, J = 1.6 Hz, 1 H), 7.83 (dd, J = 8.0, 1.6 Hz, 1 H), 7.42 (d, J = 8.0 Hz, 1 H), 3.83 (s, 3 H), 2.42 (s, 3 H), 0.24(s, 9 H). ^{13}C NMR (100 MHz, DMSO-d_6) δ 165.1, 145.1, 132.0, 129.8, 129.0, 127.4, 122.4, 102.4, 99.2, 51.8, 20.0, -0.4. LC-MS: *m/z* 247 $[M+H]^+$. To a solution of methyl 4-methyl-3-((trimethylsilyl)ethynyl)benzoate (19.7 g, 80 mmol) in CH_3OH (300 mL), and treated with K_2CO_3 (16.6 g, 120 mmol), and the mixture was stirred at room temperature for 5 minutes. The solvents were evacuated and EtOAc and H_2O were added to the residue. The organic layer was separated, and the aqueous layer was exacted with EtOAc (3×100 mL). The combined layers were dried over Na_2SO_4 and concentrated. The resulting crude was further purified by flash chromatography to give the product as a white solid(12.5 g, 90.0%). ^{1}H NMR (400 MHz, DMSO-d_6) δ 7.93 (d, J = 1.2 Hz, 1 H), 7.85 (dd, J = 8.0, 1.6 Hz, 1 H), 7.44 (d, J = 8.4 Hz, 1 H), 4.49 (s, 1H), 3.84 (s, 3 H), 2.44 (s, 3 H). ^{13}C NMR (100 MHz, DMSO-d_6) δ 165.2, 145.3, 132.3, 129.9, 129.0, 127.4, 121.9, 85.1, 80.9, 51.9, 20.1. LC-MS: *m/z* 175 $[M+H]^+$; 173 $[M-H]^-$.

Methyl 4-methyl-3-(pyrazolo[1,5-a]pyrimidin-6-ylethynyl)benzoate (10a) To a solution of **9a** (10.45 g, 60 mmol) in NMP (120 mL), 6-bromopyrazolo[1,5-a]pyrimidine (11.88 g, 60 mmol), *N, N*-diisopropylethylamine (7.76 g, 180 mmol), $Pd(PPh_3)_2Cl_2$ (0.42 g, 0.6 mmol), and CuI (0.12 g, 0.6 mmol) was placed in a vial with rubber septum. The mixture underwent 3 cycles of vacuum/filling with Ar. The mixture was stirred at 80 ℃ overnight and then quenched with H_2O. EtOAc and more H_2O were added for extraction. The combined organic layer was dried over Na_2SO_4, filtered, concentrated, and the resulting residue was purified by chromatography, giving the title compound as a white solid (14.0 g, 80.0%). ^{1}H NMR (400 MHz, DMSO-d_6) δ 9.56 (s, 1H), 8.70 (s, 1H), 8.32 (s, 1H), 8.08 (s, 1H), 7.89 (d, J= 7.6 Hz, 1H), 7.50 (d, J= 8.0 Hz, 1H), 6.82 (s, 1H), 3.86 (s, 3H), 2.56 (s, 3H). ^{13}C NMR (125 MHz, DMSO-d_6) δ 165.4, 150.9, 146.5, 146.3, 145.3, 138.2, 132.2, 130.3, 129.5, 127.6, 122.0, 104.6, 97.3, 90.2, 87.8, 52.2, 20.5. LC-MS: *m/z* 292 $[M+H]^+$.

4-Methyl-3-(pyrazolo[1,5-a]pyrimidin-6-ylethynyl)benzoic acid (11a) To a solution of **10a** (11.65 g,40 mmol) in methanol (120 mL) was added NaOH (3.2 g, 80 mmol). The mixture was stirred at 60 ℃ overnight. The mixture was acidified to pH 4 in ice bath by 5% HCl. The precipitates were filtered, washed with H_2O, and further purified by recrystallization to give the title compound as a off-white solid (10.1 g, 91.0%). ^{1}H NMR (400 MHz, DMSO-d_6) δ 13.08 (br s, 1H), 9.57 (s, 1H), 8.71 (s, 1H), 8.32 (s, 1H), 8.08 (s, 1H), 7.89 (d, *J*= 8.0 Hz, 1H), 7.49 (d, *J*= 8.0 Hz, 1H), 6.83 (s, 1H), 2.57 (s, 3H). ^{13}C NMR (125 MHz, DMSO-d_6) δ 167.0, 151.5, 147.0, 146.8, 145.3, 138.7, 132.9, 130.6, 130.3, 129.3, 122.4, 105.3, 97.8, 90.9, 88.1, 21.0. LC-MS: *m/z* 278 $[M+H]^+$; 276 $[M-H]^-$.

N-Isopropyl-4-methyl-3-(pyrazolo[1,5-a]pyrimidin-6-ylethynyl)benzamide (7a) To the suspension of 4-methyl-3-(pyrazolo[1,5-a]pyrimidin-6-ylethynyl)benzoic acid (0.28 g, 1 mmol) in CH_2Cl_2 (3 mL) was added isopropylamine (0.059 g, 1 mmol), *N, N*-diisopropylethylamine (0.39 g, 3 mmol), and PyBOP (0.62 g, 1.2 mmol). The mixture was stirred at room temperature for 6 hours. CH_2Cl_2 and H_2O were added, the organic layers were separated and the aqueous was extracted with CH_2Cl_2 (5×100 mL). The combined organic layer was dried over Na_2SO_4, filtered, and concentrated. The resulting residue was purified by flash chromatography and recrystallization, giving the title compound as a white solid (0.26 g, 81.7%). ^{1}H NMR (500 MHz, DMSO-d_6) δ 9.56 (s, 1H), 8.71 (d, *J* = 1.5 Hz, 1H), 8.33 (d, *J* = 2.0 Hz, 1H), 8.32 (d, *J* = 7.5 Hz, 1H), 8.05 (s, 1H), 7.83 (d, *J* = 8.0 Hz, 1H), 7.44 (d, *J* = 8.0 Hz, 1H), 6.84 (d, *J* = 1.5 Hz, 1H), 4.11 (sext, *J* = 7.0 Hz, 1H), 2.55 (s, 3H), 1.17 (d, *J* = 6.5 Hz, 6H). ^{13}C NMR (100 MHz, DMSO-d_6) δ 164.1, 150.6, 146.4, 146.0, 142.6, 137.7, 132.6, 130.2, 129.4, 127.8, 121.1, 104.7, 97.1, 90.8, 86.9, 40.9, 22.1 (2C), 20.0. LC-MS (ESI): *m/z* 319 $[M+H]^+$; 317 $[M-H]^-$. HRMS (ESI): *m/z* calcd for $C_{19}H_{19}N_4O$ $[M+H]^+$, 319.1553; found 319.1553. HPLC analysis: 5.23 min, 98.0%.

N-Butyl-4-methyl-3-(pyrazolo[1,5-a]pyrimidin-6-ylethynyl)benzamide (7b) Yield, 75.0%. ^{1}H NMR (500 MHz, DMSO-d_6) δ 9.56 (s, 1H), 8.70 (d, *J* = 2.0 Hz, 1H), 8.51 (t, *J* = 5.5 Hz, 1H), 8.33 (d, *J* = 2.5 Hz, 1H), 8.04 (s, 1H), 7.82 (d, *J* = 7.5 Hz, 1H), 7.45 (d, *J* = 8.0 Hz, 1H), 6.84 (d, *J* = 2.0 Hz, 1H), 3.26 (q, *J* = 6.5 Hz, 1H), 2.54 (s, 3H), 1.51 (quint, *J* = 7.5 Hz, 2H), 1.34 (sext, *J* = 7.5 Hz, 2H), 0.90 (t, *J* =

7.5 Hz, 3H). ^{13}C NMR (100 MHz, DMSO-d_6) δ 164.9, 150.7, 146.4, 146.0, 142.6, 137.7, 132.5, 130.2, 129.5, 127.7, 121.2, 104.7, 97.1, 90.8, 87.0, 31.0, 20.0, 19.4, 13.4. LC-MS (ESI): *m/z* 333 $[M+H]^+$; 331 $[M-H]^-$. HRMS (ESI): *m/z* calcd for $C_{20}H_{21}N_4O$ $[M+H]^+$, 333.1710; found 333.1708. HPLC analysis: 5.98 min, 98.6%.

N-Isobutyl-4-methyl-3-(pyrazolo[1,5-a]pyrimidin-6-ylethynyl)benzamide (7c) Yield, 70.5%. ^{1}H NMR (500 MHz, DMSO-d_6) δ 9.56 (d, *J* = 1.0 Hz, 1H), 8.70 (d, *J* = 1.5 Hz, 1H), 8.54 (t, *J* = 4.5 Hz, 1H), 8.33 (d, *J* = 2.0 Hz, 1H), 8.05 (d, *J* = 0.5 Hz, 1H), 7.83 (dd, *J* = 8.0, 1.0 Hz, 1H), 7.45 (d, *J* = 8.0 Hz, 1H), 6.83 (d, *J* = 2.0 Hz, 1H), 3.08 (t, *J* = 6.0 Hz, 2H), 2.55 (s, 3H), 1.85 (heptet, *J* = 7.0 Hz, 1H), 0.90 (d, *J* = 6.5 Hz, 6H). ^{13}C NMR (100 MHz, DMSO-d_6) δ 165.1, 150.7, 146.4, 146.0, 142.7, 137.8, 132.6, 130.2, 129.5, 127.8, 121.2, 104.7, 97.1, 90.8, 87.0, 46.6, 27.8, 20.1, 20.0 (2C). LC-MS (ESI): *m/z* 333 $[M+H]^+$; 331 $[M-H]^-$. HRMS (ESI): *m/z* calcd for $C_{20}H_{21}N_4O$ $[M+H]^+$, 333.1710; found 333.1709. HPLC analysis: 5.96 min, 99.0%.

N-Cyclohexyl-4-methyl-3-(pyrazolo[1,5-a]pyrimidin-6-ylethynyl)benzamide (7d) Yield, 67.0%. ^{1}H NMR (500 MHz, DMSO-d_6) δ 9.56 (d, *J* = 0.5 Hz, 1H), 8.71 (d, *J* = 1.5 Hz, 1H), 8.34 (d, *J* = 2.5 Hz, 1H), 8.30 (d, *J* = 8.0 Hz, 1H), 8.05 (s, 1H), 7.82 (dd, *J* = 8.0, 1.0 Hz, 1H), 7.44 (d, *J* = 8.0 Hz, 1H), 6.84 (d, *J* = 2.0 Hz, 1H), 3.80-3.72 (m, 1H), 2.55 (s, 3H), 1.86-1.70 (m, 4H), 1.64-1.58 (m, 1H), 1.35-1.26 (m, 4H), 1.18-1.08 (m, 1H). ^{13}C NMR (100 MHz, DMSO-d_6) δ 164.1, 150.7, 146.4, 146.0, 142.6, 137.8, 132.7, 130.3, 129.4, 127.9, 121.2, 104.7, 97.1, 90.8, 87.0, 48.3, 32.2 (2C), 25.1, 24.7 (2C), 20.1. LC-MS (ESI): *m/z* 359 $[M+H]^+$; 357 $[M-H]^-$. HRMS (ESI): *m/z* calcd for $C_{22}H_{23}N_4O$ $[M+H]^+$, 359.1866; found 359.1865. HPLC analysis: 6.98 min, 99.1%.

N-Cyclopentyl-4-methyl-3-(pyrazolo[1,5-a]pyrimidin-6-ylethynyl)benzamide (7e) Yield, 66.5%. ^{1}H NMR (400 MHz, DMSO-d_6) δ 9.55 (d, *J* = 1.2 Hz, 1H), 8.70 (d, *J* = 2.0 Hz, 1H), 8.37 (d, *J* = 7.2 Hz, 1H), 8.33 (d, *J* = 2.4 Hz, 1H), 8.05 (d, *J* = 1.2 Hz, 1H), 7.82 (dd, *J* = 8.0, 1.6 Hz, 1H), 7.43 (d, *J* = 8.0 Hz, 1H), 6.83 (d, *J* = 1.6 Hz, 1H), 4.26-4.20 (m, 1H), 2.54 (s, 3H), 1.92-1.88 (m, 2H), 1.70-1.68 (m, 2H), 1.58-1.53 (m, 4H). ^{13}C NMR (100 MHz, DMSO-d_6) δ 164.7, 150.7, 146.4, 146.0, 142.6, 137.8, 132.6, 130.3, 129.4, 127.9, 121.2, 104.7, 97.1, 90.9, 87.0, 50.9, 32.0 (2C), 23.5 (2C), 20.1. LC-MS

(ESI): *m/z* 345 $[M+H]^+$; 343 $[M-H]^-$. HRMS (ESI): *m/z* calcd for $C_{21}H_{21}N_4O$ $[M+H]^+$, 345.1710; found 345.1710. HPLC analysis: 6.15 min, 97.3%.

4-Methyl-N-phenyl-3-(pyrazolo[1,5-a]pyrimidin-6-ylethynyl)benzamide (7f) Yield, 83.0%. ^{1}H NMR (400 MHz, DMSO-d_6) δ10.31 (s, 1H), 9.58 (dd, *J* = 1.6, 0.4 Hz, 1H), 8.72 (d, *J* = 2.4 Hz, 1H), 8.34 (d, *J* = 2.4 Hz, 1H), 8.18 (d, *J* = 1.6 Hz, 1H), 7.95 (dd, *J* = 8.0, 1.6 Hz, 1H), 7.80 (s, 1H), 7.78 (s, 1H), 7.53 (d, *J* = 8.0 Hz, 1H), 7.36 (t, *J* = 7.6 Hz, 2H), 7.11 (t, *J* = 7.2 Hz, 1H), 6.84 (dd, *J* = 2.4, 0.8 Hz, 1H), 2.59 (s, 3H). ^{13}C NMR (125 MHz, DMSO-d_6) δ 164.4, 150.9, 146.5, 146.3, 143.6, 139.0, 138.1, 132.7, 130.8, 129.9, 128.6 (2C), 128.4, 123.7, 121.6, 120.4 (2C), 104.8, 97.3, 90.8, 87.5, 20.4. LC-MS (ESI): *m/z* 353 $[M+H]^+$; 351 $[M-H]^-$. HRMS (ESI): *m/z* calcd for $C_{22}H_{17}N_4O$ $[M+H]^+$, 353.1397; found 353.1395. HPLC analysis: 6.23 min, 99.1%.

4-Methyl-3-(pyrazolo[1,5-a]pyrimidin-6-ylethynyl)-N-(o-tolyl)benzamide (7g) Yield, 63.0%. ^{1}H NMR (400 MHz, DMSO-d_6) δ 9.97 (s, 1H), 9.58 (d, *J* = 1.2 Hz, 1H), 8.72 (d, *J* = 2.0 Hz, 1H), 8.34 (d, *J* = 2.4 Hz, 1H), 8.19 (d, *J* = 1.2 Hz, 1H), 7.96 (dd, *J* = 7.6, 1.2 Hz, 1H), 7.53 (d, *J* = 8.0 Hz, 1H), 7.34 (d, *J* = 7.2 Hz, 1H), 7.29 (d, *J* = 7.6 Hz, 1H), 7.24-7.21 (m, 1H), 7.20-7.16 (m, 1H), 6.84 (d, *J* = 1.6 Hz, 1H), 2.59 (s, 3H), 2.24 (s, 3H). ^{13}C NMR (125 MHz, DMSO-d_6) δ 164.3, 150.9, 146.5, 146.3, 143.5, 138.1, 136.3, 133.8, 132.4, 130.8, 130.3, 129.9, 128.3, 126.6, 126.0, 125.9, 121.6, 104.8, 97.3, 90.8, 87.4, 20.4, 17.9. LC-MS (ESI): *m/z* 367 $[M+H]^+$; 365 $[M-H]^-$. HRMS (ESI): *m/z* calcd for $C_{23}H_{19}N_4O$ $[M+H]^+$, 367.1553; found 367.1559. HPLC analysis: 5.80 min, 97.9%.

4-Methyl-3-(pyrazolo[1,5-a]pyrimidin-6-ylethynyl)-N-(m-tolyl)benzamide (7h) Yield, 87.5%. ^{1}H NMR (400 MHz, DMSO-d_6) δ 10.23 (s, 1H), 9.58 (d, *J* = 1.2 Hz, 1H), 8.72 (d, *J* = 2.0 Hz, 1H), 8.34 (d, *J* = 2.0 Hz, 1H), 8.17 (d, *J* = 1.2 Hz, 1H), 7.94 (dd, *J* = 8.0, 1.2 Hz, 1H), 7.63 (s, 1H), 7.59 (d, *J* = 8.0 Hz, 1H), 7.52 (d, *J* = 8.0 Hz, 1H), 7.23 (t, *J* = 8.0 Hz, 1H), 6.94 (d, *J* = 7.6 Hz, 1H), 6.84 (d, *J* = 2.0 Hz, 1H), 2.59 (s, 3H), 2.31 (s, 3H). ^{13}C NMR (125 MHz, DMSO-d_6) δ 164.3, 150.9, 146.5, 146.3, 143.5, 138.9, 138.1, 137.7, 132.7, 130.7, 129.8, 128.4, 128.3, 124.4, 121.5, 120.9, 117.6, 104.8, 97.3, 90.8, 87.4, 21.2, 20.4. LC-MS (ESI): *m/z* 367 $[M+H]^+$; 365 $[M-H]^-$. HRMS (ESI): *m/z* calcd for $C_{23}H_{19}N_4O$ $[M+H]^+$, 367.1553; found 367.1554. HPLC analysis: 7.43 min, 97.2%.

4-Methyl-3-(pyrazolo[1,5-a]pyrimidin-6-ylethynyl)-N-(p-tolyl)benzamide (7i) Yield, 90.0%. ^{1}H NMR (400 MHz, DMSO-d_6) δ 10.23 (s, 1H), 9.58 (d, J = 0.8 Hz, 1H), 8.73 (d, J = 2.0 Hz, 1H), 8.34 (d, J = 2.0 Hz, 1H), 8.17 (d, J = 1.2 Hz, 1H), 7.94 (dd, J = 8.0, 1.6 Hz, 1H), 7.67 (d, J = 8.4 Hz, 2H), 7.52 (d, J = 8.0 Hz, 1H), 7.17 (d, J = 8.4 Hz, 2H), 6.85 (d, J = 2.0 Hz, 1H), 2.59 (s, 3H), 2.28 (s, 3H). ^{13}C NMR (125 MHz, DMSO-d_6) δ 164.1, 150.9, 146.5, 146.3, 143.4, 138.1, 136.5, 132.8, 132.7, 130.7, 129.8, 129.0 (2C), 128.3, 121.5, 120.4 (2C), 104.8, 97.3, 90.8, 87.5, 20.5, 20.4. LC-MS (ESI): *m/z* 367 $[M+H]^+$; 365 $[M-H]^-$. HRMS (ESI): *m/z* calcd for $C_{23}H_{19}N_4O$ $[M+H]^+$, 367.1553; found 367.1558. HPLC analysis: 7.19 min, 99.4%.

N-(2-Chlorophenyl)-4-methyl-3-(pyrazolo[1,5-a]pyrimidin-6-ylethynyl)benzamide (7j) Yied, 52.0%. ^{1}H NMR (400 MHz, DMSO-d_6) δ 10.18 (s, 1H), 9.59 (d, J = 1.6 Hz, 1H), 8.73 (d, J = 2.0 Hz, 1H), 8.34 (d, J = 2.4 Hz, 1H), 8.20 (d, J = 1.2 Hz, 1H), 7.97 (dd, J = 8.0, 1.6 Hz, 1H), 7.59-7.56 (m, 2H), 7.55 (d, J = 8.0 Hz, 1H), 7.40 (td, J = 7.6, 1.2 Hz, 1H), 7.31 (td, J = 7.6, 1.2 Hz, 1H), 6.85 (d, J = 2.0 Hz, 1H), 2.60 (s, 3H). ^{13}C NMR (125 MHz, DMSO-d_6) δ 164.4, 150.9, 146.5, 146.3, 143.8, 138.1, 134.9, 131.8, 130.9, 130.0, 129.6, 129.5, 128.5, 128.3, 127.5, 127.4, 121.7, 104.7, 97.3, 90.7, 87.5, 20.4. LC-MS (ESI): *m/z* 387 (100%), 389 (32%) $[M+H]^+$; 385 (100%), 387 (32%) $[M-H]^-$. HRMS (ESI): *m/z* calcd for $C_{22}H_{16}ClN_4O$ $[M+H]^+$, 387.1007; found 387.1006. HPLC analysis: 7.16 min, 98.8%.

N-(3-Chlorophenyl)-4-methyl-3-(pyrazolo[1,5-a]pyrimidin-6-ylethynyl)benzamide (7k) Yield, 67.0%. ^{1}H NMR (400 MHz, DMSO-d_6) δ 10.47 (s, 1H), 9.59 (d, J = 1.6 Hz, 1H), 8.73 (d, J = 1.6 Hz, 1H), 8.34 (d, J = 2.4 Hz, 1H), 8.17 (d, J = 2.0 Hz, 1H), 7.98 (t, J = 2.0 Hz, 1H), 7.95 (dd, J = 8.0, 1.6 Hz, 1H), 7.74 (dd, J = 8.4, 1.2 Hz, 1H), 7.55 (d, J = 8.4 Hz, 1H), 7.39 (t, J = 8.4 Hz, 1H), 7.18 (dd, J = 8.0, 1.6 Hz, 1H), 6.85 (d, J = 2.0 Hz, 1H), 2.59 (s, 3H). ^{13}C NMR (100 MHz, DMSO-d_6) δ 164.4, 150.6, 146.4, 146.0, 143.6, 140.4, 137.8, 132.8, 132.2, 130.6, 130.0, 129.7, 128.2, 123.2, 121.5, 119.7, 118.5, 104.6, 97.1, 90.6, 87.4, 20.1. LC-MS (ESI): *m/z* 387 (100%), 389 (32%) $[M+H]^+$; 385 (100%), 387 (32%) $[M-H]^-$. HRMS (ESI): *m/z* calcd for $C_{22}H_{16}ClN_4O$ $[M+H]^+$, 387.1007; found 387.1006. HPLC analysis: 9.01 min, 97.8%.

N-(4-Chlorophenyl)-4-methyl-3-(pyrazolo[1,5-a]pyrimidin-6-ylethynyl)benzamide (7l) Yield, 72.0%. ^{1}H NMR (400 MHz, DMSO-d_6) δ 10.43 (s, 1H), 9.58 (d, J = 1.6 Hz, 1H), 8.73 (d, J = 2.0 Hz, 1H), 8.34 (d, J = 2.0 Hz, 1H), 8.17 (d, J = 1.6 Hz, 1H), 7.95 (dd, J = 8.0, 1.6 Hz, 1H), 7.84 (d, J = 8.8 Hz, 2H), 7.54 (d, J = 8.0 Hz, 1H), 7.43 (d, J = 8.8 Hz, 2H), 6.85 (d, J = 2.0 Hz, 1H), 2.59 (s, 3H). ^{13}C NMR (125 MHz, DMSO-d_6) δ 164.5, 150.9, 146.5, 146.3, 143.7, 138.1, 138.0, 132.4, 130.7, 129.9, 128.5 (2C), 128.4, 127.3, 121.9 (2C), 121.6, 104.7, 97.3, 90.7, 87.5, 20.4. LC-MS (ESI): *m/z* 387 (100%), 389 (32%) $[M+H]^+$; 385 (100%), 387 (32%) $[M-H]^-$. HRMS (ESI): *m/z* calcd for $C_{22}H_{16}ClN_4O$ $[M+H]^+$, 387.1007; found 387.1005. HPLC analysis: 8.83 min, 98.3%.

N-(2-Methoxyphenyl)-4-methyl-3-(pyrazolo[1,5-a]pyrimidin-6-ylethynyl)benzamide (7m) Yield, 65.0%. ^{1}H NMR (400 MHz, DMSO-d_6) δ 9.58 (d, J = 1.2 Hz, 1H), 9.56 (s, 1H), 8.73 (d, J = 2.0 Hz, 1H), 8.34 (d, J = 2.4 Hz, 1H), 8.16 (d, J = 1.6 Hz, 1H), 7.94 (dd, J = 8.0, 1.6 Hz, 1H), 7.73 (dd, J = 8.0, 1.2 Hz, 1H), 7.52 (d, J = 8.0 Hz, 1H), 7.20 (td, J = 7.2, 1.6 Hz, 1H), 7.11 (d, J = 1.6 Hz, 1H), 6.97 (td, J = 7.6, 0.8 Hz, 1H), 6.84 (d, J = 1.6 Hz, 1H), 3.84 (s, 3H), 2.59 (s, 3H). ^{13}C NMR (100 MHz, DMSO-d_6) δ 163.8, 151.4, 150.7, 146.4, 146.0, 143.3, 137.8, 132.4, 130.6, 129.7, 127.8, 126.7, 125.5, 124.1, 121.5, 120.0, 111.4, 104.7, 97.1, 90.7, 87.3, 55.6, 20.1. LC-MS (ESI): *m/z* 383 $[M+H]^+$; 381 $[M-H]^-$. HRMS (ESI): *m/z* calcd for $C_{23}H_{19}N_4O_2$ $[M+H]^+$, 383.1503; found 383.1501. HPLC analysis: 7.63 min, 99.0%.

N-(3-Methoxyphenyl)-4-methyl-3-(pyrazolo[1,5-a]pyrimidin-6-ylethynyl)benzamide (7n) Yield, 72.0%. ^{1}H NMR (400 MHz, DMSO-d_6) δ 10.28 (s, 1H), 9.58 (dd, J = 2.0, 0.8 Hz, 1H), 8.73 (d, J = 2.0 Hz, 1H), 8.34 (d, J = 2.4 Hz, 1H), 8.17 (d, J = 1.6 Hz, 1H), 7.94 (dd, J = 8.0, 1.6 Hz, 1H), 7.53 (d, J = 8.0 Hz, 1H), 7.47 (t, J = 2.0 Hz, 1H), 7.40 (dd, J = 8.0, 0.8 Hz, 1H), 7.26 (t, J = 8.0 Hz, 1H), 6.85 (dd, J = 2.0, 0.8 Hz, 1H), 6.70 (dd, J = 8.0, 2.4 Hz, 1H), 3.76 (s, 3H), 2.59 (s, 3H). ^{13}C NMR (100 MHz, DMSO-d_6) δ 164.2, 159.3, 150.7, 146.4, 146.0, 143.3, 140.0, 137.8, 132.6, 130.6, 129.6, 129.1, 128.2, 121.4, 112.5, 109.1, 106.1, 104.6, 97.1, 90.7, 87.3, 54.9, 20.1. LC-MS (ESI): *m/z* 383 $[M+H]^+$; 381 $[M-H]^-$. HRMS (ESI): *m/z* calcd for $C_{23}H_{19}N_4O_2$ $[M+H]^+$, 383.1503; found 383.1500. HPLC analysis: 6.73 min, 98.4%.

N-(4-Methoxyphenyl)-4-methyl-3-(pyrazolo[1,5-a]pyrimidin-6-ylethynyl)benzamide (7o) Yield, 86.0%. ^{1}H NMR (400 MHz, DMSO-d_6) δ 10.19 (s, 1H), 9.58 (d, J = 1.2 Hz, 1H), 8.72 (d, J = 2.0 Hz, 1H), 8.34 (d, J = 2.4 Hz, 1H), 8.16 (d, J = 1.6 Hz, 1H), 7.94 (dd, J = 8.0, 1.6 Hz, 1H), 7.69 (d, J = 8.8 Hz, 2H), 7.52 (d, J = 8.0 Hz, 1H), 6.95 (d, J = 9.2 Hz, 2H), 6.85 (d, J = 2.0 Hz, 1H), 3.75 (s, 3H), 2.58 (s, 3H). ^{13}C NMR (100 MHz, DMSO-d_6) δ 163.8, 155.5, 150.7, 146.4, 146.0, 143.1, 137.8, 132.7, 132.0, 130.5, 129.6, 128.1, 121.9 (2C), 121.4, 113.6 (2C), 104.7, 97.1, 90.7, 87.2, 55.0, 20.1. LC-MS (ESI): *m/z* 383 $[M+H]^+$; 381 $[M-H]^-$. HRMS (ESI): *m/z* calcd for $C_{23}H_{19}N_4O_2$ $[M+H]^+$, 383.1503; found 383.1498. HPLC analysis: 6.21 min, 99.1%.

N-(3-Bromophenyl)-4-methyl-3-(pyrazolo[1,5-a]pyrimidin-6-ylethynyl)benzamide (7p) Yield, 53.0%. ^{1}H NMR (400 MHz, DMSO-d_6) δ 10.44 (s, 1H), 9.58 (d, J = 1.2 Hz, 1H), 8.73 (d, J = 2.0 Hz, 1H), 8.34 (d, J = 2.4 Hz, 1H), 8.17 (d, J = 1.6 Hz, 1H), 8.11 (s, 1H), 7.95 (dd, J = 8.0, 1.6 Hz, 1H), 7.79 (d, J = 7.6 Hz, 1H), 7.55 (d, J = 8.0 Hz, 1H), 7.35-7.29 (m, 2H), 6.85 (d, J = 1.6 Hz, 1H), 2.59 (s, 3H). ^{13}C NMR (125 MHz, DMSO-d_6) δ 164.4, 150.9, 146.5, 146.3, 143.9, 140.7, 138.1, 132.3, 130.7, 130.6, 130.0, 128.4, 126.3, 122.6, 121.6, 121.4, 119.0, 104.7, 97.3, 90.7, 87.6, 20.4. LC-MS (ESI): *m/z* 431, 433 $[M+H]^+$; 429, 431 $[M-H]^-$. HRMS (ESI): *m/z* calcd for $C_{22}H_{16}BrN_4O$ $[M+H]^+$, 431.0502; found 431.0491. HPLC analysis: 8.45 min, 97.9%.

N-(3-Iodophenyl)-4-methyl-3-(pyrazolo[1,5-a]pyrimidin-6-ylethynyl)benzamide (7q) Yield, 60.0%. ^{1}H NMR (400 MHz, DMSO-d_6) δ 10.37 (s, 1H), 9.57 (d, J = 1.2 Hz, 1H), 8.72 (d, J = 2.0 Hz, 1H), 8.34 (d, J = 2.4 Hz, 1H), 8.26 (s, 1H), 8.17 (d, J = 1.2 Hz, 1H), 7.93 (dd, J = 7.6, 1.2 Hz, 1H), 7.82 (d, J = 8.0 Hz, 1H), 7.53 (d, J = 8.0 Hz, 1H), 7.47 (d, J = 7.6 Hz, 1H), 7.16 (t, J = 8.0 Hz, 1H), 6.84 (d, J = 1.6 Hz, 1H), 2.58 (s, 3H). ^{13}C NMR (100 MHz, DMSO-d_6) δ 164.5, 150.9, 146.5, 146.3, 143.8, 140.5, 138.1, 132.3, 132.2, 130.7, 130.6, 129.9, 128.4, 121.6, 119.4, 104.7, 97.3, 94.3, 90.7, 87.5, 20.4. LC-MS (ESI): *m/z* 479 $[M+H]^+$; 477 $[M-H]^-$. HRMS (ESI): m/z calcd for $C_{25}H_{16}IN_4O$ $[M+H]^+$, 479.0363; found 479.0357. HPLC analysis: 9.98 min, 98.7%.

4-Methyl-3-(pyrazolo[1,5-a]pyrimidin-6-ylethynyl)-N-(3-(trifluoromethyl)phenyl)benzamide (7r) Yield, 46.0%. ^{1}H NMR (400 MHz, DMSO-d_6) δ 10.61 (s, 1H), 9.59 (dd, J = 2.0, 0.8 Hz, 1H), 8.73 (d, J

= 2.0 Hz, 1H), 8.34 (d, *J* = 2.4 Hz, 1H), 8.25 (s, 1H), 8.20 (d, *J* = 1.6 Hz, 1H), 8.09 (d, *J* = 8.4 Hz, 1H), 7.97 (dd, *J* = 8.0, 2.0 Hz, 1H), 7.61 (t, *J* = 8.0 Hz, 1H), 7.56 (d, *J* = 8.0 Hz, 1H), 7.47 (d, *J* = 8.0 Hz, 1H), 6.85 (dd, *J* = 2.4, 0.8 Hz, 1H), 2.60 (s, 3H). ^{13}C NMR (125 MHz, DMSO-d_6) δ 164.8, 150.9, 146.5, 146.3, 144.0, 139.8, 138.1, 132.2, 130.8, 130.0, 129.8, 129.6 (q, *J* = 31.4 Hz), 128.5, 124.1 (d, *J* = 270.8 Hz), 123.7, 121.6, 120.0 (q, *J* = 3.8 Hz), 116.4 (q, *J* = 3.9 Hz), 104.7, 97.3, 90.7, 87.6, 20.4. LC-MS (ESI): *m/z* 421 $[M+H]^+$; 419 $[M-H]^-$. HRMS (ESI): *m/z* calcd for $C_{23}H_{16}F_3N_4O$ $[M+H]^+$, 421.1271; found 421.1264. HPLC analysis: 8.51 min, 99.4%.

4-Methyl-3-(pyrazolo[1,5-a]pyrimidin-6-ylethynyl)-N-(4-(trifluoromethyl)phenyl)benzamide (7s) Yield, 51.0%. ^{1}H NMR (400 MHz, DMSO-d_6) δ 10.63 (s, 1H), 9.58 (d, *J* = 1.2 Hz, 1H), 8.73 (d, *J* = 2.0 Hz, 1H), 8.34 (d, *J* = 2.4 Hz, 1H), 8.20 (d, *J* = 1.6 Hz, 1H), 8.04 (d, *J* = 8.4 Hz, 2H), 7.96 (dd, *J* = 8.0, 2.0 Hz, 1H), 7.75 (d, *J* = 8.8 Hz, 2H), 7.55 (d, *J* = 8.0 Hz, 1H), 6.85 (d, *J* = 1.6 Hz, 1H), 2.60 (s, 3H). ^{13}C NMR (125 MHz, DMSO-d_6) δ 164.8, 150.9, 146.5, 146.3, 144.0, 142.7, 138.1, 132.2, 130.8, 129.9, 128.5, 125.9 (d, *J* = 6.0 Hz, 2C), 124.3 (d, *J* = 269.5 Hz), 123.7 (d, *J* = 31.9 Hz), 121.6, 120.1 (2C), 104.7, 97.3, 90.6, 87.6, 20.4. LC-MS (ESI): *m/z* 421 $[M+H]^+$; 419 $[M-H]^-$. HRMS (ESI): *m/z* calcd for $C_{23}H_{16}F_3N_4O$ $[M+H]^+$, 421.1271; found 421.1275. HPLC analysis: 9.10 min, 98.8%.

N-(3-Isopropoxyphenyl)-4-methyl-3-(pyrazolo[1,5-a]pyrimidin-6-ylethynyl)benzamide (7t) Yield, 75.0%. ^{1}H NMR (400 MHz, DMSO-d_6) δ 10.24 (s, 1H), 9.57 (d, *J* = 1.2 Hz, 1H), 8.72 (d, *J* = 1.2 Hz, 1H), 8.33 (d, *J* = 2.0 Hz, 1H), 8.16 (d, *J* = 1.2 Hz, 1H), 7.93 (dd, *J* = 8.0, 1.6 Hz, 1H), 7.52 (d, *J* = 8.0 Hz, 1H), 7.45 (s, 1H), 7.36 (d, *J* = 8.0 Hz, 1H), 7.22 (t, *J* = 8.0 Hz, 1H), 6.84 (d, *J* = 1.6 Hz, 1H), 6.66 (dd, *J* = 8.0, 1.6 Hz, 1H), 4.56 (heptet, *J* = 6.0 Hz, 1H), 2.58 (s, 3H), 1.28 (d, *J* = 6.0 Hz, 6H). ^{13}C NMR (100 MHz, DMSO-d_6) δ 164.2, 157.5, 150.6, 146.4, 146.0, 143.3, 140.1, 137.8, 132.6, 130.6, 129.6, 129.1, 128.1, 121.4, 112.4, 111.0, 107.8, 104.7, 97.1, 90.7, 87.3, 69.2, 21.7 (2C), 20.1. LC-MS (ESI): *m/z* 411 $[M+H]^+$; 409 $[M-H]^-$. HRMS (ESI): m/z calcd for $C_{25}H_{23}N_4O_2$ $[M+H]^+$, 411.1816; found 411.1815. HPLC analysis: 8.24 min, 99.3%.

N-(3-(Dimethylamino)phenyl)-4-methyl-3-(pyrazolo[1,5-a]pyrimidin-6-ylethynyl)benzamide (7u) Yield, 72.0%. ^{1}H NMR (400 MHz, DMSO-d_6) δ 10.10 (s, 1H), 9.57 (d, *J* = 1.2 Hz, 1H), 8.72 (d, *J* = 2.0

Hz, 1H), 8.34 (d, *J* = 2.0 Hz, 1H), 8.17 (d, *J* = 1.6 Hz, 1H), 7.94 (dd, *J* = 8.0, 1.6 Hz, 1H), 7.52 (d, *J* = 8.4 Hz, 1H), 7.20-7.18 (m, 2H), 7.13 (t, *J* = 8.0 Hz, 1H), 6.84 (d, *J* = 1.6 Hz, 1H), 6.50-6.48 (m, 1H), 2.90 (s, 6H), 2.58 (s, 3H). ^{13}C NMR (100 MHz, DMSO-d_6) δ 164.3, 150.6, 146.4, 146.0, 143.6, 140.3, 137.8, 132.2, 132.0, 130.6, 130.4, 129.7, 128.4, 128.2, 121.5, 119.4, 104.6, 97.1, 93.9, 90.6, 87.3, 20.1. LC-MS (ESI): *m/z* 396 $[M+H]^+$; 394 $[M-H]^-$. HRMS (ESI): *m/z* calcd for $C_{24}H_{22}N_5O$ $[M+H]^+$, 396.1819; found 396.1817. HPLC analysis: 7.20 min, 98.5%.

N-(3-(1H-Imidazol-1-yl)phenyl)-4-methyl-3-(pyrazolo[1,5-a]pyrimidin-6-ylethynyl)benzamide (7v) Yield, 71.0%. ^{1}H NMR (400 MHz, DMSO-d_6) δ 10.51 (s, 1H), 9.58 (d, *J* = 1.6 Hz, 1H), 8.72 (d, *J* = 2.0 Hz, 1H), 8.34 (d, *J* = 2.4 Hz, 1H), 8.20 (d, *J* = 1.6 Hz, 1H), 8.19 (s, 1H), 8.06 (t, *J* = 2.0 Hz, 1H), 7.97 (dd, *J* = 8.0, 1.6 Hz, 1H), 7.80 (d, *J* = 8.8 Hz, 1H), 7.67 (s, 1H), 7.55 (d, *J* = 8.4 Hz, 1H), 7.51 (d, *J* = 8.0 Hz, 1H), 7.39 (dd, *J* = 8.0, 1.6 Hz, 1H), 7.14 (s, 1H), 6.85 (d, *J* = 1.6 Hz, 1H), 2.60 (s, 3H). ^{13}C NMR (125 MHz, DMSO-d_6) δ 164.6, 150.9, 146.5, 146.3, 143.9, 140.3, 138.1, 137.1, 135.5, 132.3, 130.7, 130.1, 130.0, 129.9, 128.4, 121.6, 118.7, 118.1, 115.9, 112.5, 104.7, 97.3, 90.7, 87.6, 20.4. LC-MS (ESI): *m/z* 419 $[M+H]^+$; 417 $[M-H]^-$. HRMS (ESI): *m/z* calcd for $C_{25}H_{19}N_6O$ $[M+H]^+$, 419.1615 ; found 419.1613. HPLC analysis: 5.99 min, 99.9%.

4-Methyl-N-(3-(4-methyl-1H-imidazol-1-yl)phenyl)-3-(pyrazolo[1,5-a]pyrimidin-6-ylethynyl)benzamide (7w) Yield, 70.0%. ^{1}H NMR (400 MHz, DMSO-d_6) δ 10.49 (s, 1H), 9.59 (s, 1H), 8.73 (d, *J* = 2.0 Hz, 1H), 8.34 (d, *J* = 2.4 Hz, 1H), 8.20 (s, 1H), 8.05 (s, 1H), 8.03 (s, 1H), 7.97 (d, *J* = 8.0 Hz, 1H), 7.75 (d, *J* = 8.4 Hz, 1H), 7.56 (d, *J* = 8.0 Hz, 1H), 7.48 (t, *J* = 8.0 Hz, 1H), 7.36 (s, 1H), 7.34 (d, *J* = 8.0 Hz, 1H), 6.85 (d, *J* = 1.6 Hz, 1H), 2.60 (s, 3H), 2.18 (s, 3H). ^{13}C NMR (125 MHz, DMSO-d_6) δ 164.6, 150.9, 146.5, 146.3, 143.9, 140.3, 138.5, 138.1, 137.2, 134.6, 132.4, 130.7, 130.0, 129.9, 128.4, 121.6, 118.3, 115.4, 114.2, 112.0, 104.7, 97.3, 90.7, 87.6, 20.4, 13.5. LC-MS (ESI): *m/z* 433 $[M+H]^+$; 431 $[M-H]^-$. HRMS (ESI): *m/z* calcd for $C_{26}H_{21}N_6O$ $[M+H]^+$, 433.1771; found 433.1769. HPLC analysis: 6.86 min, 95.6%.

4-Methyl-N-(3-((4-methylpiperazin-1-yl)methyl)phenyl)-3-(pyrazolo[1,5-a]pyrimidin-6-ylethynyl)benzamide (7x) Yield, 67.0%. ^{1}H NMR (400 MHz, DMSO-d_6) δ 10.29 (s, 1H), 9.58 (d, *J* =

1.2 Hz, 1H), 8.73 (d, *J* = 1.6 Hz, 1H), 8.34 (d, *J* = 2.4 Hz, 1H), 8.19 (s, 1H), 7.96 (d, *J* = 8.0 Hz, 1H), 7.74-7.72 (m, 2H), 7.53 (d, *J* = 8.0 Hz, 1H), 7.29 (t, *J* = 8.0 Hz, 1H), 7.03 (d, *J* = 7.6 Hz, 1H), 6.85 (d, *J* = 1.6 Hz, 1H), 3.44 (s, 2H), 2.59 (s, 3H), 2.37 (br s, 4H), 2.33 (br s, 4H), 2.15 (s, 3H). ^{13}C NMR (125 MHz, DMSO-d_6) δ 164.3, 150.9, 146.5, 146.3, 143.5, 139.0, 138.8, 138.1, 132.7, 130.7, 129.8, 128.4, 128.3, 124.2, 121.5, 120.7, 119.0, 104.8, 97.3, 90.8, 87.4, 62.2, 54.7 (2C), 52.6 (2C), 45.7, 20.4. LC-MS (ESI): *m/z* 465 $[M+H]^+$; 463 $[M-H]^-$. HRMS (ESI): *m/z* calcd for $C_{28}H_{29}N_6O$ $[M+H]^+$, 465.2397; found 465.2385. HPLC analysis: 5.82 min, 99.5%.

N-(3,5-Dimethylphenyl)-4-methyl-3-(pyrazolo[1,5-a]pyrimidin-6-ylethynyl)benzamide (7y) Yield, 85.5%. ^{1}H NMR (400 MHz, DMSO-d_6) δ 10.14 (s, 1H), 9.58 (d, *J* = 1.2 Hz, 1H), 8.72 (d, *J* = 2.4 Hz, 1H), 8.34 (d, *J* = 2.0 Hz, 1H), 8.16 (d, *J* = 1.6 Hz, 1H), 7.93 (dd, *J* = 8.0, 2.0 Hz, 1H), 7.52 (d, *J* = 8.0 Hz, 1H), 7.42 (s, 2H), 6.85 (d, *J* = 1.6 Hz, 1H), 6.75 (s, 1H), 2.58 (s, 3H), 2.27 (s, 6H). ^{13}C NMR (125 MHz, DMSO-d_6) δ 164.2, 150.9, 146.5, 146.3, 143.5, 138.8, 138.1, 137.5 (2C), 132.8, 130.7, 129.8, 128.3, 125.2, 121.5, 118.1 (2C), 104.8, 97.3, 90.8, 87.4, 21.1 (2C), 20.3. LC-MS (ESI): *m/z* 381 $[M+H]^+$; 379 $[M-H]^-$. HRMS (ESI): *m/z* calcd for $C_{24}H_{21}N_4O$ $[M+H]^+$, 381.1710; found 381.1707. HPLC analysis: 8.83 min, 95.2%.

N-(3-Chloro-5-methylphenyl)-4-methyl-3-(pyrazolo[1,5-a]pyrimidin-6-ylethynyl)benzamide (7z) Yield, 65.0%. ^{1}H NMR (400 MHz, DMSO-d_6) δ 10.37 (s, 1H), 9.58 (dd, *J* = 2.0, 0.8 Hz, 1H), 8.72 (d, *J* = 2.0 Hz, 1H), 8.34 (d, *J* = 2.4 Hz, 1H), 8.16 (d, *J* = 2.0 Hz, 1H), 7.94 (dd, *J* = 8.0, 2.0 Hz, 1H), 7.77 (s, 1H), 7.56 (s, 1H), 7.54 (d, *J* = 8.0 Hz, 1H), 7.01 (s, 1H), 6.85 (d, *J* = 1.6 Hz, 1H), 2.59 (s, 3H), 2.31 (s, 3H). ^{13}C NMR (100 MHz, DMSO-d_6) δ 164.4, 150.6, 146.4, 146.0, 143.6, 140.1, 139.8, 137.8, 132.5, 132.2, 130.6, 129.7, 128.2, 123.7, 121.5, 119.1, 116.9, 104.6, 97.1, 90.6, 87.3, 20.7, 20.1. LC-MS (ESI): *m/z* 401 (100%), 403 (32%) $[M+H]^+$; 399 (100%), 401 (32%) $[M-H]^-$. HRMS (ESI): *m/z* calcd for $C_{23}H_{18}ClN_4O$ $[M+H]^+$, 401.1164; found 401.1159. HPLC analysis: 9.86 min, 98.3%.

4-Methyl-N-(3-((4-methylpiperazin-1-yl)methyl)-5-(trifluoromethyl)phenyl)-3-(pyrazolo[1,5-a]pyrimidin-6-ylethynyl)benzamide (7ra) Yield, 40.0%. ^{1}H NMR (400 MHz, DMSO-d_6) δ 10.58 (s, 1H), 9.58 (d, *J* = 1.2 Hz, 1H), 8.73 (d, *J* = 2.0 Hz, 1H), 8.34 (d, *J* = 2.0 Hz, 1H), 8.21 (d, *J* = 6.4 Hz,

2H), 8.02 (s, 1H), 7.97 (dd, *J* = 7.6, 1.2 Hz, 1H), 7.55 (d, *J* = 8.4 Hz, 1H), 7.36 (s, 1H), 6.85 (d, *J* = 2.0 Hz, 1H), 3.54 (s, 2H), 2.59 (s, 3H), 2.40 (br s, 4H), 2.34 (br s, 4H), 2.15 (s, 3H). ^{13}C NMR (125 MHz, DMSO-d_6) δ 164.7, 150.9, 146.5, 146.3, 144.0, 140.8, 139.9, 138.1, 132.2, 130.8, 130.0, 129.2 (d, *J* = 31.1 Hz), 128.5, 124.2 (d, *J* = 270.8 Hz), 123.8, 121.6, 120.0 (d, *J* = 3.8 Hz), 115.0 (d, *J* = 3.6 Hz), 104.7, 97.3, 90.7, 87.6, 61.4, 54.6 (2C), 52.5 (2C), 45.7, 20.4. LC-MS (ESI): *m/z* 533 $[M+H]^+$; 531 $[M-H]^-$. HRMS (ESI): *m/z* calcd for $C_{29}H_{28}F_3N_6O$ $[M+H]^+$, 533.2271; found 533.2267. HPLC analysis: 11.92 min, 99.1%.

4-Methyl-N-(3-methyl-5-((4-methylpiperazin-1-yl)methyl)phenyl)-3-(pyrazolo[1,5-a]pyrimidin-6-ylethynyl)benzamide (7rb) Yield, 75.0% ^{1}H NMR (400 MHz, DMSO-d_6) δ10.21 (s, 1H), 9.58 (s, 1H), 8.73 (s, 1H), 8.34 (s, 1H), 8.18 (s, 1H), 7.94 (d, *J* = 8.0 Hz, 1H), 7.57 (s, 1H), 7.52-7.50 (m, 2H), 6.85 (s, 2H), 3.39 (s, 2H), 2.59 (s, 3H), 2.35 (br s, 8H), 2.30 (s, 3H), 2.15 (s, 3H). ^{13}C NMR (125 MHz, DMSO-d_6) δ 164.2, 150.9, 146.5, 146.3, 143.5, 138.9, 138.7, 138.1, 137.4, 132.7, 130.7, 129.9, 128.4, 125.0, 121.5, 119.5, 118.0, 104.8, 97.3, 90.8, 87.4, 62.3, 54.7 (2C), 52.6 (2C), 45.7, 21.2, 20.4. LC-MS (ESI): *m/z* 479 $[M+H]^+$; 477 $[M-H]^-$. HRMS (ESI): *m/z* calcd for $C_{29}H_{31}N_6O$ $[M+H]^+$, 479.2554; found 479.2555 . HPLC analysis: 9.67 min, 99.8%.

N-(3-Chloro-5-((4-methylpiperazin-1-yl)methyl)phenyl)-4-methyl-3-(pyrazolo[1,5-a]pyrimidin-6-ylethynyl)benzamide (7rc) Yield, 50.0%. ^{1}H NMR (400 MHz, DMSO-d_6) δ 10.44 (s, 1H), 9.58 (d, *J* = 0.8 Hz, 1H), 8.72 (d, *J* = 2.0 Hz, 1H), 8.34 (d, *J* = 2.4 Hz, 1H), 8.18 (s, 1H), 7.95-7.92 (m, 2H), 7.66 (s, 1H), 7.53 (d, *J* = 8.4 Hz, 1H), 7.07 (s, 1H), 6.84 (d, *J* = 1.6 Hz, 1H), 3.44 (s, 2H), 2.59 (s, 3H), 2.38 (br s, 4H), 2.33 (br s, 4H), 2.15 (s, 3H). ^{13}C NMR (125 MHz, DMSO-d_6) δ 164.5, 150.9, 146.5, 146.3, 143.9, 141.2, 140.3, 138.1, 132.6, 132.2, 130.8, 129.9, 128.5, 123.5, 121.6, 118.8, 118.2, 104.7, 97.3, 90.7, 87.5, 61.4, 54.7 (2C), 52.5 (2C), 45.7, 20.4. LC-MS (ESI): *m/z* 499 (100%), 501 (32%) $[M+H]^+$; 497 (100%), 499 (32%) $[M-H]^-$. HRMS: *m/z* calcd for $C_{28}H_{28}ClN_6O$ $[M+H]^+$, 499.2008; found 499.2000. HPLC analysis: 12.30 min, 99.2%.

N-(3-Methoxy-5-((4-methylpiperazin-1-yl)methyl)phenyl)-4-methyl-3-(pyrazolo[1,5-a]pyrimidin-6-ylethynyl)benzamide (7rd) Yield, 65.0%. ^{1}H NMR (400 MHz, DMSO-d_6) δ 10.26 (s, 1H), 9.59 (s, 1H),

8.73 (d, *J* = 1.6 Hz, 1H), 8.35 (d, *J* = 2.4 Hz, 1H), 8.18 (s, 1H), 7.95 (d, *J* = 8.0 Hz, 1H), 7.52 (d, *J* = 8.0 Hz, 1H), 7.42 (s, 1H), 7.34 (s, 1H), 6.85 (d, *J* = 1.6 Hz, 1H), 6.61 (s, 1H), 3.75 (s, 3H), 3.40 (s, 2H), 2.59 (s, 3H), 2.33 (br s, 8H), 2.15 (s, 3H). ^{13}C NMR (125 MHz, DMSO-d_6) δ. 164.3, 159.3, 150.9, 146.5, 146.3, 143.6, 140.1, 140.0, 138.1, 132.7, 130.7, 129.9, 128.4, 121.5, 112.9, 109.7, 104.8, 104.5, 97.3, 90.8, 87.5, 62.3, 55.0, 54.7 (2C), 52.6 (2C), 45.7, 20.4. LC-MS (ESI): *m/z* 495 $[M+H]^+$; 493 $[M-H]^-$. HRMS (ESI): *m/z* calcd for $C_{29}H_{31}N_6O_2$ $[M+H]^+$, 495.2503; found 495.2520. HPLC analysis: 8.97 min, 99.2%.

4-Methyl-N-(3-(morpholinomethyl)-5-(trifluoromethyl)phenyl)-3-(pyrazolo[1,5-a]pyrimidin-6-ylethynyl)benzamide (7re) Yield, 42.0%. ^{1}H NMR (400 MHz, DMSO-d_6) δ 10.59 (s, 1H), 9.59 (dd, *J* = 2.0, 0.8 Hz, 1H), 8.73 (d, *J* = 2.0 Hz, 1H), 8.35 (d, *J* = 2.4 Hz, 1H), 8.22 (d, *J* = 2.0 Hz, 1H), 8.20 (s, 1H), 8.04 (s, 1H), 7.98 (dd, *J* = 8.0, 1.6 Hz, 1H), 7.56 (d, *J* = 8.0 Hz, 1H), 7.38 (s, 1H), 6.85 (dd, *J* = 2.0, 0.4 Hz, 1H), 3.60 (t, *J* = 4.4 Hz, 4H), 3.56 (s, 2H), 2.60 (s, 3H), 2.40 (t, *J* = 4.4 Hz, 4H). ^{13}C NMR (125 MHz, DMSO-d_6) δ 164.7, 150.9, 146.6, 146.3, 144.0, 140.3, 139.9, 138.1, 132.1, 130.8, 130.0, 129.2 (d, *J* = 31.1 Hz), 128.5, 124.1 (d, *J* = 270.8 Hz), 123.9, 121.6, 120.1 (d, *J* = 2.5 Hz), 115.1 (d, *J* = 3.5 Hz), 104.7, 97.3, 90.7, 87.6, 66.1 (2C), 61.8, 53.1 (2C), 20.4. LC-MS (ESI): *m/z* 520 $[M+H]^+$; 518 $[M-H]^-$. HRMS (ESI): *m/z* calcd for $C_{28}H_{25}F_3N_5O_2$ $[M+H]^+$, 520.1955; found 520.1944. HPLC analysis: 9.07 min, 99.9%.

4-Methyl-N-(3-(piperidin-1-ylmethyl)-5-(trifluoromethyl)phenyl)-3-(pyrazolo[1,5-a]pyrimidin-6-ylethynyl)benzamide (7rf) Yield, 41.5%. ^{1}H NMR (400 MHz, DMSO-d_6) δ 10.58 (s, 1H), 9.58 (d, *J* = 1.2 Hz, 1H), 8.72 (d, *J* = 2.0 Hz, 1H), 8.34 (d, *J* = 2.4 Hz, 1H), 8.22 (d, *J* = 1.2 Hz, 1H), 8.19 (s, 1H), 8.01 (s, 1H), 7.97 (dd, *J* = 8.0, 1.6 Hz, 1H), 7.55 (d, *J* = 8.0 Hz, 1H), 7.35 (s, 1H), 6.85 (d, *J* = 2.0 Hz, 1H), 3.51 (s, 2H), 2.59 (s, 3H), 2.35 (br s, 4H), 1.52 (quint, *J* = 4.2 Hz, 4H), 1.42-1.38 (m, 2H). ^{13}C NMR (125 MHz, DMSO-d_6) δ 164.7, 150.9, 146.5, 146.3, 144.0, 141.1, 139.8, 138.1, 132.2, 130.8, 130.0, 129.1 (d, *J* = 31.0 Hz), 128.5, 124.2 (d, *J* = 270.6 Hz), 123.7, 121.6, 119.9 (d, *J* = 4.1 Hz), 114.9 (d, *J* = 4.9 Hz), 104.7, 97.3, 90.7, 87.5, 62.2, 53.9 (2C), 25.5 (2C), 23.9, 20.4. LC-MS (ESI): *m/z* 518

$[M+H]^+$; 516 $[M-H]^-$. HRMS (ESI): *m/z* calcd for $C_{29}H_{27}F_3N_5O$ $[M+H]^+$, 518.2162; found 518.2152. HPLC analysis: 17.6 min, 100%.

4-Methyl-3-(pyrazolo[1,5-a]pyrimidin-6-ylethynyl)-N-(3-(pyrrolidin-1-ylmethyl)-5-(trifluoromethyl) phenyl)benzamide (7rg) Yield, 40.5%. ^{1}H NMR (400 MHz, DMSO-d_6) δ 10.58 (s, 1H), 9.58 (s, 1H), 8.72 (s, 1H), 8.34 (s, 1H), 8.22 (s, 1H), 8.19 (s, 1H), 8.04 (s, 1H), 7.97 (d, *J* = 7.2 Hz, 1H), 7.55 (d, *J* = 8.0 Hz, 1H), 7.36 (s, 1H), 6.85 (s, 1H), 3.67 (s, 2H), 2.59 (s, 3H), 2.47 (br s, 4H), 1.72 (br s, 4H). ^{13}C NMR (125 MHz, DMSO-d_6) δ 164.7, 150.9, 146.5, 146.3, 144.0, 141.9, 139.8, 138.1, 132.1, 130.8, 130.0, 129.1 (q, *J* = 31.1 Hz), 128.5, 124.2 (d, *J* = 270.9 Hz), 123.5, 121.6, 119.6 (d, *J* = 4.5 Hz), 114.9 (d, *J* = 3.9 Hz), 104.7, 97.3, 90.7, 87.6, 59.0, 53.5 (2C), 23.2 (2C), 20.4. LC-MS (ESI): *m/z* 504 $[M+H]^+$; 502 $[M-H]^-$. HRMS (ESI): *m/z* calcd for $C_{28}H_{25}F_3N_5O$ $[M+H]^+$, 504.2006; found 504.1992. HPLC analysis: 13.51 min, 98.8%.

4-Ethyl-N-(3-((4-methylpiperazin-1-yl)methyl)-5-(trifluoromethyl)phenyl)-3-(pyrazolo[1,5-a]pyrimidin-6-ylethynyl)benzamide (7rh) Yield, 50.0%. ^{1}H NMR (400 MHz, DMSO-d_6) δ 10.59 (s, 1H), 9.58 (dd, *J* = 2.0, 0.8 Hz, 1H), 8.71 (d, *J* = 2.0 Hz, 1H), 8.35 (d, *J* = 2.4 Hz, 1H), 8.21 (d, *J* = 1.6 Hz, 1H), 8.20 (s, 1H), 8.02 (s, 1H), 8.00 (dd, *J* = 8.0, 2.0 Hz, 1H), 7.56 (d, *J* = 8.0 Hz, 1H), 7.36 (s, 1H), 6.85 (dd, *J* = 2.4, 0.8 Hz, 1H), 3.55 (s, 2H), 2.98 (q, *J* = 7.6 Hz, 2H), 2.40 (br s, 4H), 2.33 (br s, 4H), 2.15 (s, 3H), 1.30 (t, *J* = 7.6 Hz, 3H). ^{13}C NMR (125 MHz, DMSO-d_6) δ 164.8, 150.8, 149.7, 146.6, 146.3, 140.8, 139.9, 138.1, 132.3, 131.1, 129.2 (d, *J* = 31.5 Hz), 128.8, 128.5, 124.2 (d, *J* = 270.5 Hz), 123.8, 120.9, 120.0 (d, *J* = 2.8 Hz), 115.0 (d, *J* = 4.0 Hz), 104.7, 97.3, 90.4, 87.1, 61.4, 54.6 (2C), 52.5 (2C), 45.7, 27.0, 14.6. LC-MS (ESI): *m/z* 547 $[M+H]^+$; 545 $[M-H]^-$. HRMS (ESI): *m/z* calcd for $C_{30}H_{30}F_3N_6O$ $[M+H]^+$, 547.2428; found 547.2417. HPLC analysis: 14.05 min, 99.7%.

4-Chloro-N-(3-((4-methylpiperazin-1-yl)methyl)-5-(trifluoromethyl)phenyl)-3-(pyrazolo[1,5-a]pyrimidin-6-ylethynyl)benzamide (7ri) Yield, 45.0%. ^{1}H NMR (400 MHz, DMSO-d_6) δ 10.70 (s, 1H), 9.60 (s, 1H), 8.71 (d, *J* = 1.6 Hz, 1H), 8.36 (d, *J* = 2.4 Hz, 2H), 8.18 (s, 1H), 8.06 (dd, *J* = 8.4, 1.2 Hz, 1H), 8.00 (s, 1H), 7.84 (d, *J* = 8.4 Hz, 1H), 7.38 (s, 1H), 6.87 (d, *J* = 1.2 Hz, 1H), 3.55 (s, 2H), 2.40 (br s, 4H), 2.33 (br s, 4H), 2.15 (s, 3H). ^{13}C NMR (125 MHz, DMSO-d_6) δ 163.9, 150.7, 146.6, 146.5,

140.8, 139.6, 138.6, 137.9, 133.4, 132.5, 130.0, 129.7, 129.2 (d, J = 31.1 Hz), 124.1 (d, J = 270.6 Hz), 123.8, 121.5, 120.2 (d, J = 5.4 Hz), 115.1 (d, J = 3.8 Hz), 104.1, 97.5, 88.8, 88.5, 61.3, 54.6 (2C), 52.5 (2C), 45.7. LC-MS (ESI): *m/z* 553 $[M+H]^+$; 551 $[M-H]^-$. HRMS (ESI): *m/z* calcd for $C_{28}H_{25}ClF_3N_6O$ $[M+H]^+$, 553.1725; found 553.1718. HPLC analysis: 13.89 min, 99.5%.

N-(3-((4-Methylpiperazin-1-yl)methyl)-5-(trifluoromethyl)phenyl)-3-(pyrazolo[1,5-a]pyrimidin-6-ylethynyl)benzamide (7rj) Yield, 40.0%. ^{1}H NMR (400 MHz, DMSO-d_6) δ 10.67 (s, 1H), 9.56 (s, 1H), 8.71 (s, 1H), 8.34 (s, 1H), 8.23 (s, 1H), 8.20 (s, 1H), 8.06-8.02 (m, 2H), 7.84 (d, J = 7.6 Hz, 1H), 7.66 (t, J = 7.6 Hz, 1H), 7.37 (s, 1H), 6.84 (s, 1H), 3.55 (s, 2H), 2.40 (br s, 4H), 2.34 (br s, 4H), 2.15 (s, 3H). ^{13}C NMR (125 MHz, DMSO-d_6) δ 164.8, 150.9, 146.5, 146.3, 140.8, 139.8, 138.3, 134.9, 134.4, 130.5, 129.2 (d, J = 30.9 Hz), 129.2, 128.6, 124.1 (d, J = 270.6 Hz), 123.8, 121.8, 120.1 (d, J = 3.3 Hz), 115.0 (d, J = 3.9 Hz), 104.5, 97.3, 91.7, 83.9, 61.3, 54.6 (2C), 52.5 (2C), 45.7. LC-MS (ESI): *m/z* 519 $[M+H]^+$; 517 $[M-H]^-$. HRMS (ESI): *m/z* calcd for $C_{28}H_{26}F_3N_6O$ $[M+H]^+$, 519.2115; found 519.2107. HPLC analysis: 9.89 min, 98.4%.

Cells and reagents. The cancer cell lines (A549, NCI-H23, NCI-H460, MDA-MB-435S, MCF-7, T47D, HCT116 and K562) were purchased from ATCC and maintained as recommended by ATCC (Manassas, USA). Dasatinib and nilotinib were purchased from Biocompounds Pharmaceutical Inc. (Shanghai,China). CCK-8 was purchased from Dojindo Molecular Technologies Inc (Kumamoto, JAPAN). Dimethyl Sulfoxide (DMSO) and Cremophor were purchased from Sigma-Aldrich (Dorset, USA). D-luciferin potassium was purchased from Gold Biotechnology (St. Louis, USA). Antibodies against DDR1, p-DDR1, MMP-2 and MMP-9, respectively, were all purchased from Cell Signaling Technology Inc (Danvers, USA)

***In Vitro* Kinase Assay.** The functional assays of compounds on the kinase activities of c-kit, and Abl were determined using the FRET-based Z'-Lyte assay system according to the manufacturer's instructions (Invitrogen, USA). Tyrosine 2 Peptide was used as Abl substrate and Ser/Thr 6 peptide was used as the substrate for c-kit. The reactions were carried out in 384-well plates in a 10 μl of reaction

volume with appropriate amount of kinases in 50 mM HEPES (pH 7.5), 10 mM $MgCl_2$, 1 mM EGTA, and 0.01% Brij-35. The reactions were incubated 1 hour at room temperature in the presence of 2 μM of substrate with 10 μM of ATP (for Abl1 assays) or 300 μM of ATP (kit assay) and in the presence of various concentrations of the compounds. The development reagent was then added for further 2 hours room temperature incubation followed by the addition of stop solution. Fluorescence signal ratio of 445 nm (Coumarin)/520 nm (fluorescin) was examined on EnVision Multilabel Reader (Perkin Elmer, Inc.).

The effects of compounds on the kinases DDR1 and DDR2 were assessed by using a LanthaScreen Eu kinase activity assay technology (Invitrogen, USA). Kinase reactions are performed in a 10 μL volume in low-volume 384-well plates. The kinases in reaction buffer consists of 50 mM HEPES pH 7.5, 0.01% BRIJ-35, 10 mM MgCl2, and 1 mM EGTA, the concentration of Fluorescein-Poly GAT Substrate (Invitrogen, USA) in the assay is 100 nM, Kinase reactions were initiated with the addition of 100 nM ATP in the presence of serials of dilutions of compounds. The reactions were allowed to proceed for 1 hour at room temperature before a 10 μL preparation of EDTA (20 mM) and Eu-labeled antibody (4 nM) in TR-FRET dilution buffer are added. The final concentration of antibody in the assay well is 2 nM, and the final concentration of EDTA is 10 mM. The plate is allowed to incubate at room temperature for one more hour before the TR-FRET emission ratios of 665 nm/340 nm were acquired on a PerkinElmer EnVision Multilabel Reader (Perkin Elmer, Inc.). Data analysis and curve fitting were performed using GraphPad Prism4 software.

Active-site dependent competition binding assay- Kinomescan screening. The binding affinity of **7rh** with DDR1 was analyzed by KINOME *scan*™ system conducted by Ambit Bioscience (San Diego, USA). Briefly, kinases were tagged with DNA. The ligands were biotinylated and immobilized to streptavidin-coated beads. The binding reactions were assembled by incubating DNA-tagged kinases, immobilized ligands and test compounds in binding reactions (20% SeaBlock, 0.17×PBS, 0.05% tween-20, 6 mM DTT) for 1.0 hour at room temperature. The affinity beads were washed with washing buffer (1×PBS, 0.05% Tween-20) first and then elution buffer (1×PBS, 0.05% Tween 20, 0.5 μM non-biotinylated affinity ligands). The kinase concentration in the eluate was determined by quantitative

PCR of the DNA tagged to the kinase. The ability of the test compound to bind to the kinase was evaluated with percent control (%) as (Test compound signal – positive control signal)/ Negative control signal – positive control signal) × 100%. Negative control is DMSO control (100% Ctrl) and positive control is control compound (0 % Ctrl).

Inhibition on Cell Proliferation by MTT Assay or CCk-8 Assay. Adherent Cells were plated in 96-well culture plates with cell density of 3000-4000 cells/well and treated with indicated compounds by adding 100μL medium containing compounds of various concentrations on the second day. After 72-hour's treatment, MTT was added to each well and incubated for additional 4-5 hours, and the absorbance was measured on a microplate reader at 570nm. Cell growth inhibition was evaluated as the ratio of the absorbance of the sample to that of the control. The results are representative of at least 4 independent experiments.

Suspension cells were plated in 96-well culture plates with cell density of 5000-6000 cells/well and treated with indicated compounds by adding 100μL medium containing compounds of various concentrations on the second day. After 72-hour's treatment, CCK-8 was added to each well and incubated for additional 3-4 hours, and the absorbance was measured on a microplate reader at 450nm. Cell growth inhibition was evaluated as the ratio of the absorbance of the sample to that of the control. The results are representative of at least 4 independent experiments.

Western Blot Analysis. NCI-H23 cells were cultured in 6-well culture plates. After being serum-starved for 16-24 hours, cells were treated with of 50ug/ml collagen I and inhibitors with indicated concentration or vehicle control. After indicated period of time, western blot was carried out according to the protocol provided by Cell Signaling Technology Ltd. Briefly, cell lysates were prepared by collecting cells with 1X SDS sample buffer (62.5 mM Tris-HCl , pH 6.8, 2% w/v SDS, 10% glycerol, 50 mM DTT, 0.01% w/v bromophenol blue). After being sonicated and boiled, cell lysates containing 10-20ug proteins were loaded to 8% or 15% SDS PAGE gel. Separated proteins were then transferred to a PVDF film. After blocked with 1X TBS containing 0.1% Tween-20 and 5% non-fat milk at 4℃

overnight, the film was incubated first with corresponding primary antibody at 4℃ overnight, then with HRP-labeled secondary antibody at room temperature for 1 hour. And the protein lanes were visualized by using ECL Western Blotting Detection Kit (Thermo Scientific. USA) according to the manufacture's instruction.

Apoptosis Analysis by Flow Cytometry. NCI-H23 cells were seeded in 6-well plates and were treated with compounds under indicated concentrations for 24 hours. The apoptosis assay was performed with Annexin-V/7-AAD Apoptosis Detection Kit according to the manufacturer's instructions. Briefly, cells were harvested, washed with ice-cold PBS, and then stained with annexin-V-FITC and 7-AAD for 15 minutes at room temperature in the dark. Stained cells were analyzed with a FACS Calibur Flow Cytometer. Annexin-V(-)/7-AAD(-) cells were classified as live cells; Annexin-V(+)/7-AAD(-) cells were classified as early apoptotic cells; Annexin-V(+)/7-AAD(+) cells were classified as late apoptotic or necrotic cells ; AnnexinV(-) and 7-AAD(+) cells were classified as dead cells.

Cell Adhension Assay. Pre-coated 48 well plate with BD Matrigel at 37℃ for 2 hours. Single cell suspension were prepared in 2% FBS RPMI-1640 medium. Then seed cells with DMSO control or compounds at a density of 1×10^5 cells/well. After 1-2 hrs of incubation at 37℃, the cells were washed with PBS to remove the non-adherent cells. Adherent cells were fixed and stained with 0.1% crystal violet in 96% ethanol. To obtain the adherent cell number, stained cells were extracted with 30% HAC and measured the absorbance at 570 nm.

Cell Invasion Assay. The tests were carried out with Transwell polycarbonate inserts (Merck Millipore, pore size 8.0 μm) in 24-well plates. Briefly, after pre-coated with BD Matrigel at 37℃ for 2 hours, the liquid was removed, and unspecific binding was blocked by 100 μL of 1% BSA. After 30 min, it was washed once with PBS. Then 6×10^4 NCI-H23 cells in 2% RPMI-1640 FBS medium with compound or control were seeded onto the upper chamber and 10% RPMI-1640 FBS medium with compound or control was added to the lower wells. After 24h's treatment, cells were fixed and stained

with 6% glutaraldehyde and 0.4% Crystal violet at room temperature for 30 min. After 30 min, the cells were washed with PBS. Then removed cells in the upper chamber cotton swabs .Pictures were taken using an invert photomicroscope.

Colony Formation Assay. NCI-H23 cells were trypsinized and counted, 400 cells were seeded in 6-well plates and different concentration of **7rh** and **7rj** were added. At least four replicate were set. After incubation for 10 days, the cells were washed with PBS, fixed with glutaraldehyde, and stained with crystal violet. The number of macroscopic colonies per dish was counted and the IC_{50} was calculated with GraphPad Prism 5.0. For soft agarose colony assay, 0.7ml 1.2% low melting agarose and 0.7ml 2x RPMI 1640 were mixed and injected in 6-well plate as bottom agarose, 0.6ml 0.6% low melting agarose and 0.6ml 2x RPMI 1640 with 400 cells were mixed and added as upper agarose. After incubation for 10 days, image was collected using microscope with camera.

Pharmacokinetics study. Compounds **7rh** and **7rj** were dissolved in mixed solvents (DMSO : EtOH: Cremophor EL : H_2O = 2 : 4 : 4 : 90) as clear solution. The final concentrations were 2.5 mg/mL. Sprague Dawley (SD) rats (male, 4 animals per group) weighted 180~220g were injected intravenously or administrated orally at doses of 5 mg/kg (i.v.) or 25mg/kg (p.o.), respectively. After dose administration, 0.3 mL of the orbital blood was taken at 2.0 min, 10.0 min, 30.0 min, 1.0 h, 2.0 h, 3.0 h, 4.0 h, 6.0 h, 8.0 h, 12.0 h, 21.0 h, 24.0 h, 30.0 h, 36.0 h, 48.0 h, and 72.0 h. Samples were stored at -70℃ until shipment to the analytical laboratory and tested by HPLC/MS using propranolol as internal standard to measure the compound concentration in the blood. The pharmacokinetics parameters were calculated using DAS (Drug and Statistics) 2.0 software (Mathematical Pharmacology Professional Committee of China, Shanghai, China). [41]

ACKNOWLEDGMENT

We thank National Basic Research Program of China (# 2010CB529706, 2009CB940904), National Natural Science Foundation (# 21072192), Key Project on Innovative Drug of Guangdong province (# 2011A080501013), Strategic Collaborative project of Guangdong province and Chinese Academy of

Sciences, Key Project on Innovative Drug of Guangzhou City (grant # 2009Z1-E911, 2010J-E551), and the grant from Chinese Academy of Sciences (CAS) for their financial support.

ABBREVIATION: DDR, discoidin domain receptor; RTK, receptor tyrosine kinase; NSCLC, non-small cell lung cancer; siRNA, small interference RNA; SCC, squamous lung cancer; MMP, matrix metalloproteinase; ECM, extracellular matrix; RNA, ribonucleic acid; IC_{50}, half maximal (50%) inhibitory concentration of a substance; Abl, abelson; Src, sarcoma; Lyn, v-yes-1 Yamaguchi sarcoma viral related oncogene homologue; c-Kit, mast/stem cell growth factor receptor; VEGFR, vascular endothelial growth factor receptor; Btk, Bruton Tyrosine Kinase; EphA3, ephrin A3; Bcr-Abl, break point cluster region-abelson receptor; TEA, triethylamine; NMP, *N*-methyl-2-pyrrolidone; PyBOP, benzotriazol-1-yl-oxytripyrrolidinophosphonium hexafluorophosphate; DIPEA, *N, N*-diisopropylethylamine; DCM, dichloromethane; ATP, adenosine triphosphate; FRET, fluorescence resonance energy transfer; Ras, rat sarcoma; Raf, rapidly accelerated fibrosarcoma; Erk, Extracellular signal regulated kinase; PI3K, phosphoinositide-3-kinase; Bcl-xL, B-cell lymphoma-extra large; CML, chronic myelogenous leukaemia; AUC, area under concentration-time curve; $T_{1/2}$, half-life period; T_{max}, peak time; C_{max}, peak concentration; F, fraction of bioavailability; I.V., intravenous; TLC, thin-layer chromatography; TMS, tetramethylsilane; ppm, parts per million; HPLC, high performance liquid chromatography; DMSO, dimethyl sulfoxide; EGTA, ethylene glycol tetraacetic acid; GAT, glycine-alanine-threonine; EDTA, ethylene diamine tetraacetic acid; MTT, (3-(4,5-dimethylthiazol-2-yl)-2,5-diphenyltetrazolium bromide; SDS, sodium-dodecyl sulphate; DTT, dithiothreitol; TBS, Tris-buffered saline; PVDF, polyvinylidene fluoride; ECL, enhanced chemoluminescence; FITC, fluorescein isothiocyanate; 7-AAD, 7-aminoactinomycin; FBS, fetal bovine serum; BSA, bovine serum albumin; HEPES, 4-(2-hydroxyethyl)-1-piperazineethanesulfonic acid, S-score, selectivity score.

SUPPORTING INFORMATION

Synthesis and chemical data for the key intermediates, ^{1}HNMR spectrum and purity determination for compound **7a**-**7rj**, apoptosis induced by compounds **7rh** and **7rj**, quantity analysis of the results from invasion assay, colon formation assay, and anti-proliferative data of the other compounds. This material is available free of charge *via* the Internet at http://pubs.acs.org..

REFERENCES

1. Johnson, J. D.; Edman, J. C. and Rutter. W. J. A receptor tyrosine kinase found in breast carcinoma cells has an extracellular discoidin I-like domain. *Proc. Natl. Acad. Sci. USA* **1993**, 90, 5677-5681.

2. Alves, F.; Vogel, W.; Mossie, K.; Millauer, B.; Höfler, H.; Ullrich A. Distinct structural characteristics of discoidin I subfamily receptor tyrosine kinases and complementary expression in human cancer. *Oncogene* **1995**, *10*, 609-618.

3. Vogel, W.; Discoidin damain receptors: structural relations and functional implication. *FASEB J.* **1999**, *13*, S77-S82.

4. Vogel, W.; Gish, G. D.; Alves, F.; Pawson, T. The discoidin domain receptor tyrosine kinases are activated by collagen. *Mol. Cell* **1997**, *1*, 13-23

5. Shrivastava, A.; Radziejewski, C.; Campbell, E.; Kovac, L.; McGlynn, M.; Ryan, T. E.; Davis, S.; Goldfarb, M. P.; Glass, D. J.; Lemke, G.; Yancopoulos, G. D. An orphan receptor tyrosine kinase family whose members serve as nonintegrin collagen receptors. *Mol. Cell* **1997**, *1*, 25-34.

6. Ram, R.; Lorente, G.; Nikolich, K.; Urfer, R.; Foehr, E.; Nagavarapu U. Discoidin domain receptor-1a (DDR1a) promotes glioma cell invasion and adhesion in association with matrix metalloproteinase-2. *J. Neurooncol.* **2006**, *76*, 239-248.

7. Hou, G.; Vogel, W. F.; Bendeck, M. P. Tyrosine kinase activity of discoidin domain receptor 1 is necessary for smooth muscle cell migration and matrix metalloproteinase expression. *Circ. Res.* **2002**, 90, 1147-1149.

8. Agarwal, G.; Mihai, C.; Iscru, D. F. Interaction of discoidin domain receptor 1 with collagen type 1. *J. Mol. Biol.* **2007**, 367, 443-455.

9. Valiathan, R. R.; Marco, M.; Leitinger, B.; Kleer, C. G. and Fridman, R. Discoindin domain receptor tyrosine kinases: new players in cancer progression. *Cancer Metastasis Rev.* **2012**, 31, 295-321.

10. Radiola, I. Discoidin domainreceptors role in human disease. *Not. Sci. Biol.* **2011**, *3*, 07-12.

11. Vogel, W. F.; Abdulhussein, R.; and For C. F. Sensing extracellular matrix: an update on discoidin domain receptor fuction. *Cell. Signal.* **2006**, *18*, 1108-1116.

12. Yang, S. H.; Baek, H. A.; Lee, H. J.; Park, H. S.; Jang, K. Y.; Kang, M. J.; Lee, D. G.; Lee, Y. C.; Moon, W. S.; Chung, M. J. Discoidin domain receptor 1 is associated with poor prognosis of non-small cell lung carcinomas. *Oncol. Rep.* **2010**, *24*, 311-319.

13. Park, H. S.; Kim, K. R.; Lee, H. J.; Choi, H. N.; Kim, D. K.; Kim, B. T.; Moon, W. S. Overexpression of discoidin domain receptor 1 increases the migration and invasion of hepatocellular carcinoma cells in association with matrix metalloproteinase. *Oncol. Rep.* **2007**, *18*, 1435–1441.

14. Yoshida, D.; Teramoto, A. Enhancement of pituitary adenoma cell invasion and adhesion is mediated by discoidin domain receptor-1. *J. Neurooncol.* **2007**, *82*, 29–40.

15. Shimada, K.; Nakamura, M.; Ishida, E.; Higuchi, T.; Yamamoto, H.; Tsujikawa, K.; Konishi, N. Prostate cancer antigen-1 contributes to cell survival and invasion though discoidin receptor 1 in human prostate cancer. *Cancer Sci.* **2008**, *99*, 39–45.

16. (a) Ford, C. E.; Lau, S. K.; Zhu, C. Q.; Andersson, T.; Tsao, M. S.; Vogel, W. F. Expression and mutation analysis of the discoidin domain receptors 1 and 2 in non-small cell lung carcinoma. *Br. J. Cancer* **2007**, *96*, 808–814. (b) Rikova, K.; Guo, A.; Zeng, Q.; Possemato, A.; Yu, J.; Haack, H.; Nardone, J.; Lee, K.; Reeves, C.; Li, Y.; Hu, Y.; Tan, Z.; Stokes, M.; Sullivan, L.; Mitchell, J.; Wetzel, R.; Macneill, J.; Ren, J. M.; Yuan, J.; Bakalarski, C. E.; Villen, J.; Kornhauser, J. M.; Smith, B.; Li, D.;

Zhou, X.; Gygi, S. P.; Gu, T. L.; Polakiewicz, R. D.; Rush, J.; Comb, M. J. Global survey of phosphotyrosine signaling identifies oncogenic kinases in lung cancer. *Cell* **2007**, *131*, 1190–1203. (c) Davies, H.; Hunter, C.; Smith, R.; Stephens, P.; Greenman, C.; Bignell, G.; Teague, J.; Butler, A.; Edkins, S.; Stevens, C.; Parker, A.; O'Meara, S.; Avis, T.; Barthorpe, S.; Brackenbury, L.; Buck, G.; Clements, J.; Cole, J.; Dicks, E.; Edwards, K.; Forbes, S.; Gorton, M.; Gray, K.; Halliday, K.; Harrison, R.; Hills, K.; Hinton, J.; Jones, D.; Kosmidou, V.; Laman, R.; Lugg, R.; Menzies, A.; Perry, J.; Petty, R.; Raine, K.; Shepherd, R.; Small, A.; Solomon, H.; Stephens, Y.; Tofts, C.; Varian, J.; Webb, A.; West, S.; Widaa, S.; Yates, A.; Brasseur, F.; Cooper, C. S.; Flanagan, A. M.; Green, A.; Knowles, M.; Leung, S. Y.; Looijenga, L. H.; Malkowicz, B.; Pierotti, M. A.; the, B. T.; Yuen, S. T.; Lakhani, S. R.; Easton, D. F.; Weber, B. L.; Goldstraw, P.; Nicholson, A. G.; Wooster, R.; Stratton, M. R.; Futreal, P. A. Somatic mutations of the protein kinase gene family in human lung cancer. *Cancer Res.* **2005**, *65*, 7591–7595. (d) Ding, L.; Getz, G.; Wheeler, D. A.; Mardis, E. R.; McLellan, M. D.; Cibulskis, K.; Sougnez, C.; Greulich, H.; Muzny, D. M.; Morgan, M. B.; Fulton, L.; Fulton, R. S.; Zhang, Q.; Wendl, M. C.; Lawrence, M. S.; Larson, D. E.; Chen, K.; Dooling, D. J.; Sabo, A.; Hawes, A. C.; Shen, H.; Jhangiani, S. N.; Lewis, L. R.; Hall, O.; Zhu, Y.; Mathew, T.; Ren, Y.; Yao, J.; Scherer, S. E.; Clerc, K.; Metcalf, G. A.; Ng, B.; Milosavljevic, A.; Gonzalez-Garay, M. L.; Osborne, J. R.; Meyer, R.; Shi, X.; Tang, Y.; Koboldt, D. C.; Lin, L.; Abbott, R.; Miner, T. L.; Pohl, C.; Fewell, G.; Haipek, C.; Schmidt, H.; Dunford-Shore, B. H.; Kraja, A.; Crosby, S. D.; Sawyer, C. S.; Vickery, T.; Sander, S.; Robinson, J.; Winckler, W.; Baldwin, J.; Chirieac, L. R.; Dutt, A.; Fennell, T.; Hanna, M.; Johnson, B. E.; Onofrio, R. C.; Thomas, R. K.; Tonon, G.; Weir, B. A.; Zhao, X.; Ziaugra, L.; Zody, M. C.; Giordano, T.; Orringer, M. B.; Roth, J. A.; Spitz, M. R.; Wistuba, II.; Ozenberger, B.; Good, P. J.; Chang, A. C.; Beer, D. G.; Watson, M. A.; Ladanyi, M.; Broderick, S.; Yoshizawa, A.; Travis, W. D.; Pao, W.; Province, M. A.; Weinstock, G. M.; Varmus, H. E.; Gabriel, S. B.; Lander, E. S.; Gibbs, R. A.; Meyerson, M.; Wilson, R. K. Somatic mutations affect key pathways in lung adenocarcinoma. *Nature* **2008** *455*, 1069–1075.

17. (a) Barker, K. T. ; Martindale, J. E. ; Mitchell, P. J. ; Kamalati, T. ; Page, M. J. ; Phippard, D. J. ; Dale, T. C. ; Gusterson, B. A. ; Crompton, M. R. Expression patterns of the novel receptor-like tyrosine kinase, DDR, in human breast tumours. *Oncogene* **1995***, 10*, 569–575. (b) Neuhaus, B., Buhren, S.; Bock, B.; Alves, F.; Vogel, W. F.; Kiefer, F. Migration inhibition of mammary epithelial cells by Syk is blocked in the presence of DDR1 receptors. *Cellular and Molecular Life Sciences: CMLS*. **2011**, *68*, 3757-3770. (c) Turashvili, G.; Bouchal, J.; Baumforth, K.; Wei, W.; Dziechciarkova, M.; Ehrmann, J.; Klein, J.; Fridman, E.; Skarda, J.; Srovnal, J.; Hajduch, M.; Murray, P.; Kolar, Z. Novel markers for differentiation of lobular and ductal invasive breast carcinomas by laser microdissection and microarray analysis. *BMC Cancer* **2007**, *7*, 55.

18. (a) Weiner, H. L.; Rothman, M.; Miller, D. C.; Ziff, E. B. Pediatric brain tumors express multiple receptor tyrosine kinases including novel cell adhesion kinases. *Pediatr. Neurosurg.* **1996** *25*, 64–71. (b) Weiner, H. L.; Huang, H.; Zagzag, D.; Boyce, H.; Lichtenbaum, R.; Ziff, E. B. Consistent and selective expression of the discoidin domain receptor-1 tyrosine kinase in human brain tumors. *Neurosurgery* **2000,** *47*, 1400–1409. (c) Ram, R.; Lorente, G.; Nikolich, K.; Urfer, R.; Foehr, E.; Nagavarapu, U. Discoidin domain receptor-1a (DDR1a) promotes glioma cell invasion and adhesion in association with matrix metalloproteinase-2. *J. Neurooncol.* **2006,** *76*, 239–248. (d) Yamanaka, R.; Arao, T.; Yajima, N.; Tsuchiya, N.; Homma, J.; Tanaka, R.; Sano, M.; Oide, A.; Sekijima, M.; Nishio, K. Identification of expressed genes characterizing long-term survival in malignant glioma patients. *Oncogene* **2006**, *25*, 5994–6002. (e) Yoshida, D.; Teramoto, A. Enhancement of pituitary adenoma cell invasion and adhesion is mediated by discoidin domain receptor-1. *J. Neurooncol.* **2007**, *82*, 29–40.

19. (a) Heinzelmann-Schwarz, V. A.; Gardiner-Garden, M.; Henshall, S. M.; Scurry, J.; Scolyer, R. A.; Davies, M. J.; Heinzelmann, M.; Kalish, L. H.; Bali, A.; Kench, J. G.; Edwards, L. S.; Vanden Bergh P. M.; Hacker, N. F.; Sutherland, R. L.; O'Brien, P. M. Overexpression of the cell adhesion molecules DDR1, Claudin 3, and Ep-CAM in metaplastic ovarian epithelium and ovarian cancer. *Clin. Cancer Res.* **2004**, *10*, 4427–4436. (b) Quan, J.; Yahata, T.; Adachi, S.; Yoshihara, K.; and Tanaka, K. (2011).

Identification of receptor tyrosine kinase, discoidin domain receptor 1 (DDR1), as a potential biomarker for serous ovarian cancer. *Int. J. Mol. Sci.* **2011**, *12*, 971-982. c) Colas, E.; Perez, C.; Cabrera, S.; Pedrola, N.; Monge, M.; Castellvi, J.; Eyzaguirre, F.; Gregorio, J.; Ruiz, A.; Llaurado, M.; Rigau, M.; Garcia, M.; Ertekin, T.; Montes, M.; Lopez-Lopez, R.; Carreras, R.; Xercavins, J.; Ortega, A.; Maes, T.; Rosell, E.; Doll, A.; Abal, M.; Reventos, J.; Gil-Moreno, A. Molecular markers of endometrial carcinoma detected in uterine aspirates. *Int. J. Cancer* **2011**, *129*, 2435–2444.

20. (a) Squire, J. A.; Bayani, J.; Luk, C.; Unwin, L.; Tokunaga, J.; MacMillan, C.; Irish, J.; Brown, D.; Gullane, P.; Kamel-Reid, S. Molecular cytogenetic analysis of head and neck squamous cell carcinoma: By comparative genomic hybridization, spectral karyotyping, and expression array analysis. *Head Neck* **2002**, *24*, 874–887. (b) Hidalgo-Carcedo, C.; Hooper, S.; Chaudhry, S. I.; Williamson, P.; Harrington, K.; Leitinger, B.; Sahai, E. Collective cell migration requires suppression of actomyosin at cell-cell contacts mediated by DDR1 and the cell polarity regulators Par3 and Par6. *Nat. Cell Biol.* **2011**, *13*, 49-58.

21. (a) Shen, Q.; Cicinnati, V. R.; Zhang, X.; Iacob, S.; Weber, F.; Sotiropoulos, G. C.; Radtke, A.; Lu, M.; Paul, A.; Gerken, G.; Beckebaum, S. Role of microRNA-199a-5p and discoidin domain receptor 1 in human hepatocellular carcinoma invasion. *Mol. Cancer* **2010**, *9*, 227. b) Gu, T. L.; Deng, X.; Huang, F.; Tucker, M.; Crosby, K.; Rimkunas, V.; Wang, Y.; Deng, G.; Zhu, L.; Tan, Z.; Hu, Y.; Wu, C.; Nardone, J.; MacNeill, J.; Ren, J.; Reeves, C.; Innocenti, G.; Norris, B.; Yuan, J.; Yu, J.; Haack, H.; Shen, B.; Peng, C.; Li, H.; Zhou, X.; Liu, X.; Rush, J.; Comb, M. J. Survey of tyrosine kinase signaling reveals ROS kinase fusions in human cholangiocarcinoma. *PloS One* **2011,** *6*, e15640.

22. Couvelard, A.; Hu, J.; Steers, G.; O'Toole, D.; Sauvanet, A.; Belghiti, J.; Bedossa, P.; Gatter, K.; Ruszniewski, P.; Pezzella, F. Identification of potential therapeutic targets by gene-expression profiling in pancreatic endocrine tumors. *Gastroenterology* **2006,** *131*, 1597–1610.

23. (a) Valencia, K.; Ormazabal, C.; Zandueta, C.; Luis-Ravelo, D.; Anton, I.; Pajares, M. J.; Agorreta, J.; Montuenga, L. M.; Martínez-Canarias, S.; Leitinger, B.; Lecanda, F. Inhibition of collagen receptor discoidin domain receptor-1 (DDR1) reduces cell survival, homing and colonization in lung cancer bone metastasis. *Clin. Cancer Res*. **2012**, *18*, 969-980. (b) Das, S.; Ongusaha, P. P.; Yang, Y. S.; Park, J. M.; Aaronson, S. A.; Lee, S. W. Discoidin domain receptor 1 receptor tyrosine kinase induces cyclooxygenase-2 and promotes chemoresistance through nuclear factor-kappaB pathway activation. *Cancer Res.* **2006**, *66,* 8123-8130. (c) Kim, H. G.; Hwang, S. Y.; Aaronson, S. A.; Mandinova, A.; Lee, S. W. DDR1 receptor tyrosine kinase promotes prosurvival pathway through Notch1 activation. *J. Biol. Chem.* **2011,** *286*, 17672-17681.

24. (a) Hammerman, P. S.; Sos, M. L.; Ramos, A. H.; Xu. C.; Dutt, A.; Zhou, W.; Brace, L. E.; Woods, A. A.; Lin, W.; Zhang, J.; Deng, X.; Lim, S. M.; Heynck, S.; Peifer, M.; Simard, J. R.; Lawrence, M. S.; Onofrio, R. C.; Salvesen, H. B.; Seidel, D.; Zander, T.; Heuckmann, J. M.; Soltermann, A.; Moch, H.; Koker, M.; Leenders, F.; Gabler, F.; Querings, S.; Ansén, S.; Brambilla, E.; Brambilla, C.; Lorimier, P.; Brustugun, O. T.; Helland, A.; Petersen, I.; Clement, J. H.; Groen, H.; Timens, W.; Sietsma, H.; Stoelben, E.; Wolf, J.; Beer, D. G.; Tsao, M. S.; Hanna, M.; Hatton, C.; Eck, M. J.; Janne, P. A.; Johnson, B. E.; Winckler, W.; Greulich, H.; Bass, A. J.; Cho, J.; Rauh, D.; Gray, N. S.; Wong, K.-K. Haura, E. B.; Thomas, R. K. and Meyerson, M. Mutations in the DDR2 kinase gene identify a novel therapeutic target in squamous cell lung cancer. *Cancer Discov.* **2011***, 1*, 78–89. (b) Ohashi, K.; Pao, W. A new target for therapy in squamous cell carcinoma of the lung. *Cancer Discov.* **2011**, *1*, 23-24. (c) Drilon, A.; Rekhtman, N.; Ladanyi, M.; Paik, P. Squamous-cell carcinomas of the lung: emerging biology, controversies, and the promise of targeted therapy. *Lancet Oncol.* **2012**, *13*, e418-e426.

25. (a) Rix, U.; Hantschel, O.; Durnberger, G.; Remsing Rix, L. L.; Planyavsky, M.; Fernbach, N. V.; Kaupe, I.; Bennett, K. L.; Valent, P.; Colinge, J.; Köcher, T.; Superti-Furga, G. Chemical proteomic profiles of the BCR-ABL inhibitors imatinib, nilotinib, and dasatinib reveal novel kinase and nonkinase

targets. *Blood* **200,** *110*, 4055–4063. (b) Bantscheff, M.; Eberhard, D.; Abraham, Y.; Bastuck.; S.; Boesche, M.; Hobson, S.; Mathieson, T.; Perrin, J.; Raida, M.; Rau, C.; Reader, V.; Sweetman, G.; Bauer, A.; Bouwmeester, T.; Hopf, C.; Kruse, U.; Neubauer, G.; Ramsden, N.; Rick, J.; Kuster, B.; Drewes, G. Quantitative chemical proteomics reveals mechanisms of action of clinical ABL kinase inhibitors. *Nat. Biotechnol.* **2007,** *25*, 1035–1044. (c) Hantschel, O.; Rix, U.; and Superti-Furga, G. Target spectrum of the BCR-ABL inhibitors imatinib, nilotinib and dasatinib. *Leuk. Lymphoma.* **2008,** *49*, 615–619. (d) Day, E.; Waters, B.; Spiegel, K.; Alnadaf, T.; Manley, P. W.; Buchdunger, E.; Walker, C.; Jarai, G. Inhibition of collagen-induced discoidin domain receptor 1 and 2 activation by imatinib, nilotinib and dasatinib. *Eur. J. Pharmacol.* **2008,** *599*, 44–53. (e) Li, J.; Rix, U.; Fang, B.; Bai, Y.; Edwards, A.; Colinge, J.; Bennett, K. L.; Gao, J.; Song, L.; Eschrich, S.; Superti-Furga, G.; Koomen, J.; Haura, E. B. A chemical and phosphoproteomic characterization of dasatinib action in lung cancer. *Nat. Chem. Biol.* **2010**, *6*, 291–299.

26. Rix, U.; Remsing Rix, L. L.; Terker, A. S.; Fernbach, N. V.; Hantschel, O.; Planyavsky, M.; Breitwieser, F. P.; Herrmann, H.; Colinge, J.; Bennett, K. L.; Augustin, M.; Till, J. H.; Heinrich, M. C.; Valent, P.; Superti-Furga, G. A. Comprehensive target selectivity survey of the BCR-ABL kinase inhibitor INNO-406 by kinase profiling and chemical proteomics in chronic myeloid leukemia cells. *Leukemia* **2010**, *24*(1), 44–50.

27. Kotz, J. The DDR is in. *SciBX* **2011**, 4, 1-2. doi:10.1038/scibx.2011.559

28. Kumar, R.; Crouthamel. M.-C.; Rominger, D. H.; Gontarek, R. R.; Tummino, P. J.; Levin,R. A. and King, A. G. Myelosuppression and kinase selectivity of multikinase angiogenesis inhibitors. *Br. J. Cancer*. **2009**, 101, 1717–1723.

29. Sun, X.; Phan, T. N.; Jung, S. H.; Kim, S. Y.; Cho, J. U.; Lee, H.; Woo, S. H.; Park, T. K.; Yang, B. S. LCB 03-0110, a novel pan-DDR/c-Src family tyrosine kinase inhibitor, suppresses scar formation by inhibiting fibroblast and macrophage activation. *J. Pharmacol. Exp. Ther.* **2012**, 340, 510-519.

20. Chinchilla, R.; Najera, C. The Sonogashira reaction: a booming methodology in synthetic organic chemistry. *Chem. Rev.* **2007,** *10*, 874-922.

31. The assay was conducted by following the protocol from the agent manufactory (https://perkinelmerreagents.onconfluence.com).

32. (a) Zhou, T.; Commodore, L.; Huang, W. S.; Wang, Y.; Thomas, M.; Keats, J.; Xu, Q.; Rivera, V. M.; Shakespeare, W. C.; Clackson, T.; Dalgarno, D. C.; Zhu, X. Structural mechanism of the pan-BCR-ABL inhibitor ponatinib (AP24534): lessons for overcoming kinase inhibitor resistance. *Chem. Biol. Drug Des.* **2011**, *77*, 1-11; (b) Huang, W.-S.; Metcalf, C. A.; Sundaramoorthi, R.; Wang, Y.; Zou, D.; Thomas, R. M.; Zhu, X.; Cai, L.; Wen, D.; Liu, S.; Romero, J.; Qi, J.; Chen, I.; Banda, G.; Lentini, S. P.; Das, S.; Xu, Q.; Keats, J.; Wang, F.; Wardwell, S.; Ning, Y.; Snodgrass, J. T.; Broudy, M. I.; Russian, K.; Zhou, T.; Commodore, L.; Narasimhan, N. I.; Mohemmad, Q. K.; Iuliucci, J.; Rivera, V. M.; Dalgarno, D. C.; Sawyer, T. K.; Clackson, T. and Shakespeare, W. C. Discovery of 3-[2-(Imidazo[1,2-b]pyridazin-3-yl)ethynyl] -4-methyl-N-{4-[(4-methylpiperazin-1-yl) methyl]-3-(trifluoromethyl)phenyl} benzamide (AP24534), a Potent, Orally Active Pan-Inhibitor of Breakpoint Cluster Region-Abelson (BCR-ABL) Kinase Including the T315I Gatekeeper Mutant. *J. Med. Chem.*, **2010**, *53*, 4701–4719. (c) Li, Y.; Shen, M.; Zhang, Z.; Luo, J.; Pan, X.; Lu, X.; Long, H.; Wen, D.; Zhang, F.; Leng, F.; Li, Y.; Tu , Z.; Ren, X. and Ding, K. Design, Synthesis, and Biological Evaluation of 3-(1H-1,2,3-Triazol-1-yl)benzamide Derivatives as Potent Pan Bcr-Abl Inhibitors Including the Threonine315→Isoleucine315 Mutant. *J. Med. Chem.* **2012**, *55,*10033–10046.

33. (a) Chetoui, N. ; El Azreq, M. A. ; Boisvert, M. ; Bergeron, M. E.; and Aoudjit, F. Discoidin domain receptor 1 expression in activated T cells is regulated by the ERK MAP kinase signaling pathway. *J. Cell. Biochem.* **2011**, *112*, 3666–3674. (b) Ongusaha, P. P.; Kim, J. I.; Fang, L.; Wong, T. W.; Yancopoulos, G. D.; Aaronson, S. A.; Lee, S. W. p53 induction and activation of DDR1 kinase counteract p53-mediated apoptosis and influence p53 regulation through a positive feedback loop. *EMBO J.* **2003**, *22*, 1289–1301.

34. (a) Shelling, A. N.; Butler, R.; Jones, T,.; Laval, S.; Boyle, J. M.; Ganesan, T. S. Localization of an epithelial-specific receptor kinase (EDDR1) to chromosome 6q16. *Genomics* **1995**, 25, 584-587. (b) Hou, G.; Vogel, W.; Bendeck, M. P. The discoidin domain receptor tyrosine kinase DDR1 in arterial wound repair. *J. Clin. Invest.* **2001**, 107, 727-735.

35. (a) Itoh, Y.; Nagase, H. Matrix metalloproteinases in cancer. *Essays Biochem.* **2002**, *38*, 21-36. (b) Roy, R.; Yang, J.; Moses, A. M. Matrix metalloproteinases as novel biomarkers and potential therapeutic targets in human cancer. *J. Clin. Oncol.* **2009**, *27*, 5287–5297. (c) Kessenbrock, K.; Plaks, V.; Werb, Z. Matrix metalloproteinases: regulators of the tumor microenvironment. *Cell* **2010**, *141*, 52–67.

36. (a) Aimes, R. T.; Quigley, J. P. Matrix metalloproteinase-2 is an interstitial collagenase. Inhibitor-free enzyme catalyzes the cleavage of collagen fibrils and soluble native type I collagen generating the specific 3/4- and 1/4-length fragments. *J. Biol. Chem.* **1995**, 270, 5872-5876. (b) Fridman, R.; Toth, M.; Chvyrkova, I.; Meroueh, S. O.; Mobashery, S. Cell surface association of matrix metalloproteinase-9 (gelatinase B). *Cancer Metastasis Rev.* **2003**, 22, 153-166. (c) Pellikainen, J. M.; Ropponen, K. M.; Kataja, V. V.; Kellokoski, J. K.; Eskelinen, M. J.; Kosma, V. M. Expression of matrix metalloproteinase (MMP)-2 and MMP-9 in breast cancer with a special reference to activator protein-2, HER2, and prognosis. *Clin. Cancer Res.* **2004**, 15, 7621–7628. (d) Roomi, M. W.; Monterrey, J. C.; Kalinovsky, T.; Rath, M.; Niedzwiecki, A. Patterns of MMP-2 and MMP-9 expression in human cancer cell lines. *Oncol. Rep.* **2009**, 21, 1323-1333.

37. Chen, H. C. Boyden chamber assay. *Methods Mol. Biol.* **2005**, 294, 15-22.

38. Gumbiner, B. MCell adhesion: The molecular basis of tissue architecture and morphogenesis. *Cell* **1996**, *84*, 345-357.

39. (a) Gross, O.; Beirowski, B.; Harvey, S. J.; McFadden, C.; Chen, D.; Tam, S.; Thorner, P. S.; Smyth, N.; Addicks, K.; Bloch, W.; Ninomiya, Y.; Sado, Y.; Weber, M. and Vogel, W. F. DDR1-

deficient mice show localized subepithelial GBM thickening with focal loss of slit diaphragms and proteinuria. *Kidney Intl.* **2004**, *66*, 102-111. (b) Curat, C. A.; Vogel, W. F. Discoidin domain receptor 1 controls growth and adhesion of mesangial cells. *J. Am. Soc. Nephrol.* **2002**, 13, 2648-2656. (c) Yeh, Y.-C.; Wu, C.-C.; Wang, Y.-K.; and Tang, M.-J. DDR1 triggers epithelial cell differentiation by promoting cell adhesion through stabilization of E-cadherin. *Mol. Biol. Cell.* **2011**, *22*, 940–953. (d) L'hôte, C. G.; Thomas, P. H.; Ganesan, T. S. Functional analysis of discoidin domain receptor 1: effect of adhesion on DDR1 phosphorylation. *FASEB J.* **2002**, *16*, 234-236.

40. Humphries, M. J. Cell adhesion assays. *Methods Mol. Biol.* **2009**, 522, 203-210.

41. (a) Song, N.; Zhang, S.; Li, Q.; Liu, C. Establishment of a liquid chromatographic/mass spectrometry method for quantification of tetrandrine in rat plasma and its application to pharmacokinetic study. *J. Pharmaceut. Biomed. Anal.* **2008**, *48*, 974–979. (2) Li, Y.; Zhang, Y.; Wang, S.; Zhu, J.; Tian, Y.; Chen, B. Quantitative analysis of atractylenolide I in rat plasma by LC–MS/MS method and its application to pharmacokinetic study. *J. Pharmaceut. Biomed. Anal.* **2012**, *58*, 172–176.

42. (a) Pichot, C. S.; Harting, S. M.; Xia, L.; Arvanitis, C.; Monisvais, D.; Lee, F. Y.; Frost, J. A.; and Corey, S. J. Dasatinib synergizes with doxorubicin to block growth, migration and invation of breast cancer cells. *Brit. J. Cancer* **2009**, *101*, 38-47. (b) Huang, F.; Reeves, K.; Han, X.; Fairchild, C.; Platero, S.; Wong, T. W.; Lee, F.; Shao, P.; and Clark, E. Identifation of candidate molecula markers predicting sensitivity in solide tumor to dasatinib: rationale for patient selection. *Cancer Res.* **2007**, *67*, 2226-2238. (c) Serrels, A.; Macpherson, I. R. J.; Evans, T. R. J.; Lee, F. Y.; Clark, E. A.; Sansom, O. J.; Ashton, G. H.; Frame, M. C.; and Brunton, V. G. *Mol.* Identification of potential biomarkers for measuring inhibition of Src kinase activity in colon cancer cells following treatment with dasatinib. *Cancer Ther.* **2006**, *5*, 3014-3022.

43. Dejmek, J.; Leandersson, K.; Manjer, J.; Bjartell, A.; Emdin, S. O.; Vogel, W. F.; Landberg, G.; Andersson, T. Expression and signaling activity of Wnt-5a/discoidin domain receptor-1 and Syk plays distinct but decisive roles in breast cancer patient survival. *Clin Cancer Res.* **2005**, 11, 520-528.

Table of Contents graphic